PLASMA-SHEATH-WALL TIME-DEPENDENT BEHAVIOR: AN INFORMAL SURVEY

by

Charles K. Birdsall

Memorandum No. UCB/ERL M82/51

22 June, 1982

Electronics Research Laboratory
University of California
Berkeley, CA 94720

Research sponsored by the Department of Energy, Contract DE-AS03-76ET53064
and Office of Naval Research, Contract N00014-77-C-0578.

Plasma-Sheath-Wall Time-Dependent Behavior

An Informal Survey

Charles K. Birdsall

Abstract There is evidence that plasma-sheath-wall interactions include large amplitude collective behavior, at low and high frequencies. This report is a loose collection of such evidence, covering theory, simulations and experiments.

Introduction

Plasmas interact with bounding walls in a variety of ways in various configurations. These interactions involve sheaths, virtual cathodes, double layers, self-biasing, and the areas of plasma chemistry and plasma processing. The configurations range from tiny Langmuir probes to discharges used in plasma cleaning, etching, sputterings, deposition et al., to first walls in fusion devices. Some of these interactions exhibit large potential fluctuations ($e\phi >> KT$) and or collective effects, at low through to high frequencies (e.g. ω_p).

Evidence of time dependent plasma-wall behavior grows persistently and needs further understanding. This survey consists of a list of representative publications, followed by cut outs from articles with notations. These were prepared for transparencies for an informal siminar on plasma sheaths and large plasma potentials held at Biwa-ko, Japan November 20, 21, 1981, led by Dr. H. Ikegami. Much of the material has puzzled and stimulated me for decades. The reason for binding these is simply the recurring need to refer co-workers to these works. The list is incomplete, does not sort out definitive works and is not for journal submission. Additions and corrections will be appreciated.

Some Highlights

Attention is called to a number of clear cut observations of fluctuations at high frequencies, meaning near ω_p.

Tien and Moshman (1956), using particle computer simulations, observed a peak in shot noise near $(\omega_p)_{minimum}$ for a thermionic diode, electrons only; Rousset and Birdsall, same model, (1981, on-going work) have some evidence of

$\phi_{minimum}$, $x_{minimum}$ oscillations near ω_{pe}. Birdsall and Bridges, also using simulations (1961, 1963, 1966), found large amplitude oscillations of the virtual cothode, near ω_{pe}, for a cold electron beam in a diode at currents larger than "maximum", with substantial differences between the average of the time-dependent results and time-independent analysis.

Dunn and Ho (1963) with electron-ion particle simulation of open circut plasma diodes (for space propulsion) found an oscillating electron sheath provided just the electron current needed for neutralization.

Cutler (1964) observed low and high frequency oscillations in a cesium plasma diode, short-circuited, in the ratio of $\sqrt{m_e/m_i}$. High frequency bursts always occur slightly before the onset of the low-frequency current pulses. The supposition is that drifting electrons cause an instability [Birdsall and Bridges electron diode type or Pierce electron-ion ($m_i \to \infty$) diode type (1944) or electron beam-plasma type] which decreases the average electron current; relaxation of the resultant charge imbalance produces a cycle of the ion oscillation. Burger (1964) saw similar effects in simulations, claiming that dc states do not exist in collisionless plasma diodes; Burger (1965) provides more details, showing large relaxation-type amplitude oscillations in current and potential, with frequencies characteristic of the ions. Cutler and Burger (1966) put experiments and simulations together, showing large amplitude oscillations at frequencies corresponding to ion transit times, with high frequency bursts during parts of these fluctuations.

These articles (plus others) are selected to provide evidence of low and high frequency large amplitude fluctuations in various plasma-wall devices. This information excites the imagination about the behavior of other plasma-wall configurations. Are there always electron bursts (at ω_p) followed by ion relaxation oscillations? Do such excite large amplitude waves (BGK, soliton, electron hole), which propagate (or damp) away from the wall as sound- or fluid- or particle- or pseudo- waves?

Certainly, laboratory and simulation experimentalists are encouraged to examine high and low frequency spectra and especially to look for possible bursts near ω_{pe} followed by relaxations near ω_{pi}.

Attention is called to the analysis of Cipolla and Silveitch (1968) on temporal formation of a plasma sheath at an absorbing floating wall, using Boltzmann electrons ($m_e \to 0$) and cold fluid ions. They find that a dipole pulse (oriented to accelerate ions toward the wall) moves into the plasma, with v_{group} decreasing toward v_{sound}, and spreading (hence, not a linear sound wave). Thus, there is formation of a "natural" sheath ($n_i > n_e$, width a few λ_D near the wall) and a Bohm presheath (width of 10's of λ_D), in this nonlinear solution.

I am currently using the same model, but with particle electrons and ions with simulations done to date with T. Kamimura and Y. Ohara at IPP, Nagoya, Japan. We can report so far, for $T_e >> T_i$ having non-zero m_e produces large $e\phi_{wall}/KT_e$ oscillations at ω_p; the edge of the region of large ion acceleration and decrease in N_e, N_i and T_e, propagates away from the wall at v_{sound}, with ion wall collection at speeds between v_s and $2v_s$. For $T_i \approx T_e$, the ion collection is spread over $f(v_{ti})$, centered on v_{ti}. Much remains to be done; progress will appear in our Berkeley progress reports.

Since the Biwa-ko seminar, a number of additions have been made to the references, accounting for some breaks in the year by year listings. Special reference to some of these is given, following.

Self-biasing of open circuited walls at plasma boundaries, that is, setting up floating potentials has been known since Langmuir or earlier, but is still being studied (e.g., our simulation model described above). Self-biasing also occurs when low frequency rf fields are capacitively coupled to a discharge, leading to ion acceleration to the wall, as treated by Sturrock (1959) and Butler and Kino (1963). This mechanism is thought to provide ion acceleration in the parallel-plate capacitively-coupled rf discharges now widely used in plasma etching of integrated circuits. [These papers were provoked in part by experiments done by myself and A. J. Lichtenberg (1959) attempting plasma confinement at low frequency which we had misinterpreted. Our rf slow-wave focusing was later understood and made to work at high frequency on an electron beam, by G. Rayfield and myself (1964).]

Double layers have been studies extensively, in space, in the laboratory and in simulations. This name conjures up a model of a dipole charge layer

with a potential jump. The physics described is a plasma region downstream from an electron source where there is a potential drop which is relatively stable and large ($e\phi/KT >> 1$) causing most electrons to be reflected back toward their source. This behavior suggests the alternative name of virtual cathode which is also associated with limiting currents and the possibility of low and high frequency oscillations (a la Birdsall and Bridges, Cutler and Burger). The papers by N. Sato and K. Saeki and their co-authors deserve careful reading. The report by Hollenstein et al. (1980) (first read by me March 1982) shows localized stationary potential jumps with $e\phi KT_e >> 1$ and, indeed, with a spectrum of high frequency fluctuations centered about f_{pe} with a fullwidth of 0.3 f_{pe}, and a localized increase of T_e. It would be interesting to learn whether Hollenstein et al. observed pulses of a few to many cycles at f_{pe} (bursts in time) and whether these triggered (were followed by) activity at lower frequencies associated with ion sound or ions transit time effects.

Ion bursts due to pulsing a grid with small to large potentials at $f \approx f_{pi}$ are observed in simulations by Estabrook and Alexeff (1972), using Vlasov ions and Boltzmann electrons ($m_e \to 0$). The bursts are ballistic (kinetic) in nature, (not ion sound) little affected by the self consistent fields (hence, called pseudowaves), extending on the order of $10\lambda_D$ into the plasma, at velocities up to about 4 v_s. For a grid held negative (at $e\phi/KT_e = -2$) Estabrook et al. (1971) found the ion distribution is almost flat extending to about ± 1.8 v_s. These large ion velocities near a negative grid are similar to those observed in our particle simulations with an absorbing floating wall.

In laboratory or computer experiments, some clues as to causes and effects are obtained from spectral measurements. Random particle noise with a flat spectrum, white noise, is commonly called shot noise. Spectra which are not flat, but have peaks and valleys etc., indicate that resonant or collective effects may be occurring. The current spectra of Tien and Moshman (1956) clearly demonstrate the low frequency smoothing of shot noise by the dynamics of the potential minimum (the Deybe cloud) in front of a thermionic emmitter, an effect known since the 1930's; the peak near $\omega = \omega_p$ shown by Tien and Moshman is the overcompensation for shot noise found by Whinnery (1954); the "Tien dip" just below the peak is open to question. The large oscillations in potential minima obtained by Birdsall and Bridges (1961, 1963, 1966) for cold beams beyond limiting currents are resonances at frequencies related to transit times at the plasma

frequency (i.e., $\frac{\omega_p^L}{V} = \omega_p^T = n\pi$); such couple power to external loads poorly and so must be probed carefully, perhaps by the capacitive probes of Hollenstein et al. (1980). The spectral clues found by Cutler and Burger (1966) at low and high frequencies were important in unravelling the physics.

Double layers in the laboratory may be set up by applying large potential differences across a plasma. In space, in the auroral problem, a current is applied to the system, leading to instabilities which tend to form holes in ion phase space which evolve into multiple $e\phi/KT_e \approx 1$ double layers, as described by Hudson and Potter (1981) and others.

Acknowledgments

The informal seminar on plasma sheaths and plasma potentials planned for November 20, 21, 1981 at Biwa-ko, Japan provoked me into listing papers which I had known many years earlier and commenting on a few in order to bring out the time-dependent nature of these. I am grateful to Dr. T. Kamimura, my host at the Institute of Plasma Physics, Nagoya University, Nagoya Japan (Sept. 1, 1981 to February 28, 1982) who helped set up the seminar, and Dr. H. Ikegami who chaired the meetings and stimulated the discussions. I am grateful to Drs. H. Kakihana and Y.H Ichikawa for maintaining an excellent library at IPP which made finding papers easy, and librarians who searched and copied for me. I am grateful to Drs. N. Sato and K. Saeki of Tohoku University for discussions at Biwa-ko and Sendai on their double layer observations and for their papers which stimulated some of my later simulations, especially those exploring the possible ties between large amplitude sheath fluctuations and excitation of large amplitude waves. I am grateful to Drs. R. W. Gould and W. B. Bridges, my hosts at California Institute of Technology (March 1 to September 1, 1982) where the text has been added to the seminar bibliography and transparencies.

PLASMA SHEATHS, DYNAMIC BEHAVIOR; a listing of references.

1925 Langmuir, I., Scattering of electrons in ionized gases, Phys. Rev. 26, 585-613.

1929 Tonks, L., and Langmuir, I., Oscillations in ionized gases, Phys. Rev. 33, 195-210, February.

1939 Merrill, H.J., and Webb, H.W., Electron Scattering and Plasma Oscillations, Phys. Rev. 55, 1191-1198, June.

1956 Tien, P.K., and Moshman, J., Monte Carlo calculation of noise near the potential minimum of a high-frequency diode, J. Appl. Phys. 27, 1067-1078, September.

1959 Auer, P.L., and Hurwitz, H. Jr., Space charge neutralization by positive ions in diodes, J. Appl. Phys. 30, 161-165, February.

1960 Auer, P.L., Potential distributions in a low-pressure thermionic converter, J. Appl. Phys. 31, 2096-2103, December.

1961 Birdsall, C.K., and Bridges, W.B., Space-charge instabilities in electron diodes and plasma converters, J. Appl. Phys. 32, 2611-2618, December,

1963 Butler, H.S., and Kino, G.S., Plasma sheath formation by radio-frequency fields, Phys. Fluids 6, 1346-1355, September.

Bridges, W.B., Space-charge instabilities in electron diodes. II, J. Appl. Phys. 34, 2946-2955, October.

Dunn, D.A., and Ho, I.T., Computer experiments on Ion-beam neutralization with initially cold electrons, AIAA J. 1, 2770-2777, December.

1964 Cutler, W.H., High-frequency oscillations in a thermal plasma, J. Appl. Phys. 35, 464-465.

Burger, P., Nonexistence of dc states in low-pressure thermionic converters, J. Appl. Phys. 35, 3048-3049.

Norris, W.T., Nature of spontaneous oscillations in a cesium diode energy converter, J. Appl. Phys. 35, 3260-3268, November.

1965 Burger, P., Theory of large-amplitude oscillations in the one-dimensional low-pressure cesium thermionic converter, J. Appl. Phys. 36, 1938-1943, June.

Burger, P., Dunn, D.A., and Halsted, A.S., Computer experiments on the randomization of electrons in a collisionless plasma, Phys. Fluids 8, 2263-2272, December.

1966 Brown, S.C., "Introduction to electrical discharges in gases", see especially Chapter 18, Plasma oscillations, Wiley, NY.

Cutler, W.H., and Burger, P., Oscillations in the thermal cesium plasma diode, J. Appl. Phys. 37, 2867-2873, June.

1967 Burger, P., Zero-field solutions and their stability in the one-dimensional low-pressure cesium diode, J. Appl. Phys. 38, 3360-3368, July.

1968 Hockney, R.W., Formation and stability of virtual electrodes in a Cylinder, J. Appl. Phys. 39, 4166-4170, August.

1969 Alexeff, I., Jones, W.D., Lonngren, K., and Montgomery, D., Transient plasma sheath—discovered by ion-acoustic waves, Phys. Fluids 12, 345-346, February.

1970 Widner, M., Alexeff, I., Jones, W.D., and Lonngren, K.E., Ion acoustic wave excitation and ion sheath evolution, Phys. Fluids 13, 2532-2540, October.

1979 Michelsen, P., Pécseli, H.L., Juul Rasmussen, J. and Schrittwieser, R., The current-driven, ion-acoustic instability in a collisionless plasma, Plasma Phys. 21, 61-73.

Kuhn, S., Determination of axial steady-state potential distributions in collisionless single-ended Q-machines, Plasma Phys. 21, 613-626.

1981 Cipolla, Jr., J.W., and Silevitch, M.B., On the temporal development of a plasma sheath, J. Plasma Phys. 25, 373-389, June.

Garrett, H.B., Neutralizing charged-up spacecraft, IEEE spectrum, 44-47, July.

Kuhn, S., Phelps, A.D.R., and Fang, M.T.C., Low-frequency longitudinal instability in collisionless single-ended Q machines, Phys. Fluids 24, 1586-1587, August.

1961 Sellen Jr., J. M. and Shelton, H., "Electrostatic Propulsion", see especially, Transient and Steady State Behavior in Cesium Ion Beams, 305-356, Academic Press.

1963 Buneman, O., and Kooyers, G., Computer Simulation of the Electron Mixing Mechanism in Ion Propulsion, AIAA J. 1, 2525-2528, November.

1964 Derfler, H., Nonexistence of Quiescent Plasma States in Ion Propulsion, Phys. Fluids 7, 1625-1637, October.

1965 Wadhwa, R. P., Buneman, O., and Brauch, D. F., Two-Dimensional Computer Experiments on Ion-Beam Neutralization, AIAA J. 3, 1076-1081, June.

1971 Dunn, D. A., "Models of Particles and Moving Media", see especially Chapter 6.7, The Two-Species Diode with Infinite Spacing—Ion Propulsion Beam Neutralization, 219-226, Academic Press.

1954 Whinnery, J.R., Noise phenomena in the region of the potential minimum, IRE Trans. Electron Devices, ED-1 Part 4, 221-237.

1959 Sturrock, P.A., Interpretation of the results of the rf confinement experiment, Microwave Lab., Rep. No. 638, W.W. Hansen Lab of Physics, Stanford Univ., Stanford, CA, October.

1964 Gould, R.W., Excitation of ion-acoustic waves, Phys. Rev. 136, No. 4A, A991-A997, 16 November.

Rayfield, G.W. and C.K. Birdsall, Focussing of an electron stream with radio frequency fields, Jour. Elec. and Control, 17, 601-622, December.

1966 Birdsall, C.K. and W.B. Bridges, Electron dynamics of diode regions, Academic Press. (see Chapter 3).

1968 Hirshfield, J.L. and J.H. Jacob. Free-streaming and spatial landau damping, Phys. Fl. 11, No. 2, February.

1971 Estabrook, K., M. Widner, I. Alexeff and W.D. Jones, Simulation of pseudowaves and of plasma sheath formation about a grid by computer solution of the Vlasov equation, Phys. Fl. 14, 1792-1794, August.

1972 Estabrook, K. and I. Alexeff, Simulation of ion acoustic wave and pseudowave generation in a plasma, Phys. Fl., 15, 2026-2033, November.

1982 Nightingale, I.L., E.R. Ault and A.A. Mondelli, One-dimensional static sheath characteristics, J. Appl. Phys. 53, 886-890, February.

PLASMA DOUBLE LAYERS AND LARGE PLASMA POTENTIALS; a list of references.

1974 Knorr, G., and Goertz, C.K.,Existence and stability of strong potential double layers, Astrophys. Space Sci. 31, 209-223.

1975 Goertz, C.K., and Joyce, G., Numerical simulation of the plasma double layers, Astrophys. Space Sci. 32, 165-173.

1977 DeGroot, J.S., Barnes, C., Walstead, A.E., and Buneman, O., Localized structures and anomalous dc resistivity, Phys. Rev. Lett. 38, 1283-1286, May.

1978 Joyce, G., and Hubbard, R.F., Numerical simulation of plasma double layers, J. Plasma Phys. 20, 391-404, December.

1979 Hubbard, R.F., and Joyce, G., Simulation of auroral double layers, J. Geophys. Res., 84, 4297.

1980 Singh, N., Computer experiments on the formation and dynamics of electric double layers, Plasma Phys., 22, 1, 1980.

Singh, N., Kist, R., and Thiemann, H., and Block, L.P., Experimental and numerical studies on potential distributions in a plasma, Plasma Phys., 22, 695-707.

Levine, J.S., and Crawford, F.W., A fluid description of plasma double-layers, J. Plasma Phys. 23, 223-247.

Johnson, L.E., Numerical model of plasma double layers using the Vlasov equation, J. Plasma Phys. 23, 433-452, June.

Wagner, J.S., Tajima, T., Kan, J.R., Leboeuf, J.N., Akasofu, S.-I., and Dawson, J.M., V-Potential double layers and the formation of auroral arcs, Phys. Rev. Lett., 45, 803.

Sato. T., and Okuda, H., Ion acoustic double layers, Phys. Rev. Lett., 44, 740.

1981 Sato, T., and Okuda, H., Numerical simulations on ion acoustic double layers, J. Geophys. Res., 86, 3357.

Baker, K.D., Singh, N., Block, L.P., Kist, R., Kampa, W., and Thiemann, H., Studies of strong laboratory double layers and comparison with computer simulation, J. Plasma Phys. 26, 1-27.

Hudson, M.K., and Potter, D.W., Electrostatic shocks in the auroral magnetosphere, in Auroral Arcs, AGU Geophysical Monograph 25,

1979 Schamel, H., Theory of electron holes, Physica Scripta, Vol. 20, 336-342.

Lynov, J.P., P. Michelsen, H.L. Pecseli, J.J. Rasmussen, K. Saeki and V.A. Turikov, Observations of solitary structures in a magnetized, plasma loaded waveguide, Physica Scripta, Vol. 20, 328-335.

Saeki, K., P. Michelsen, H.L. Pecseli and J.J. Rasmussen, Formation and coalescence of electron solitary holes, Phys. Rev. Letters, Vol. 42, No. 8, February 19.

Iizuka, S., K. Saeki, N. Sato and Y. Hatta, Buneman instability, Pierce instability, and double-layer formation in a collisionless plasma, Vol. 43, No. 19, November 5, Phys. Rev. Lett.

1980 Benjamin, N.M.P., Plasma turbulence in a "Q" machine, Ph.D. thesis, Keble College, Oxford University.

Lynov, J.P., P. Michelsen, H.L. Pecseli and J.J. Rasmussen, Interaction between electron holes in a strongly magnetized plasma, Vol. 80A, No. 1, November 10, Phys. Lett.

Hollenstein, Ch., M. Guyot and E.S. Weibel, Stationary potential jumps in a plasma, LRP 165/80, Ecole Polytechnique Federale de Lausanne - Suisse, February.

Saeki, K., S. Iizuka and N. Sato, Ion heating due to double-layer disruption in a plasma, Phys. Rev. Letters, Vol. 45, No. 23, December 8.

1981 Sato, N., R. Hatakeyama, S. Iizuka, T. Mieno, K. Saeki, J.J. Rasmussen and P. Michelsen, Stationary double layers in a non-discharge magnetoplasma, Dept. of Electronic Engineering, Tohoku Univ., 980.Sendai, Japan, April 1.

Sato, N., R. Hatakeyama, S. Iizuka, T. Mieno and K. Saeki, Ultrastrong stationary double layers in a nondischarge magnetoplasma, Phys. Rev. Letters, Vol. 46, No. 20, May 18.

DOUBLE-LAYER EXPERIMENTS OF N. HERSHKOWITZ et al.

1978 Coakley, P., N.Hershkowitz, R.Hubbard, and G.Joyce
"Experimental observations of strong double-layers"
Phys. Rev. Letters 40, 230 January.

1979 Coakley, P., L.Johnson and N.Hershkowitz "Strong laboratory double-layers in the presence of a magnetic field" Physics Letters 70A, 425 April.

Coakley, P. and N. Hershkowitz "Laboratory double layers"
Phys. Fluids 22, 1171 June.

1981 Hershkowitz, N. "Double layers and electrostatic shocks"
Jour. Geophys. Res. 86, 3307-3310 May.

Chan, C., N.Hershkowitz, and G.L.Payne "Laboratory double layers with no external fields" Physics Letters 83A(7), 328 June.

Hershkowitz, N., G.L.Payne, C.Chan, and J.R.DeKock
"Weak double layers" Plasma Physics 23, 903 October.

Coakley, P. and N.Hershkowitz "Moving double layers"
Physics Letters 83A, 131 .

PLASMA EXPANSION INTO A VACUUM; a list of references.

1970 Allen, J.E., and Andrews, J.G., A note on ion rarefaction waves, J. Plasma Phys. 4, 187-194, February.

1971 Widner, M., Alexeff, I., and Jones, W.D., Plasma Expansion into a vacuum, Phys. Fluids 14, 795-796, April.

1975 Crow, J.E., Auer, P.L., and Allen, J.E., The expansion of a plasma into a vacuum, J. Plasma Phys. 14, 65-76, August.

1978 Wickens, L.M., Allen, J.E., and Rumsby, P.T., Ion emission from laser-produced plasmas with two electron temperatures, Phys. Rev. Lett. 41, 243-246, July.

1979 Denavit, J., Collisionless plasma expansion into a vacuum, Phys. Fluids 22, 1384-1392, July.

Lonngren, K.E., Quasi-neutral plasma expansion: A fluid model approach, IEEE Trans. Plasma Sci. PS-7, 232-233, December.

Mora, P., and Pellat, R., Self-similar expansion of a plasma into a vacuum, Phys. Fluids 22, 2300-2304, December.

1980 Denavit, J., Time filtering particle simulations with $\omega_{pe}\Delta t >> 1$, UCRL-85097 preprint.

1981 Holm, D.D., Johnson, S.F., and Lonngren, K.E., Expansion of a cold ion cloud, Appl. Phys. Lett. 38, 519-521, April.

True, M.A., Albritton, J.R., and Williams, E.A., Fast ion production by suprathermal electrons in laser fusion plasmas, Phys. Fluids 24, 1885-1893, October.

ELECTRON DIODE, Warm emitter

JOURNAL OF APPLIED PHYSICS VOLUME 27, NUMBER 9 SEPTEMBER, 1956

Monte Carlo Calculation of Noise Near the Potential Minimum of a High-Frequency Diode

P. K. TIEN AND J. MOSHMAN
Bell Telephone Laboratories, Murray Hill, New Jersey
(Received March 22, 1956)

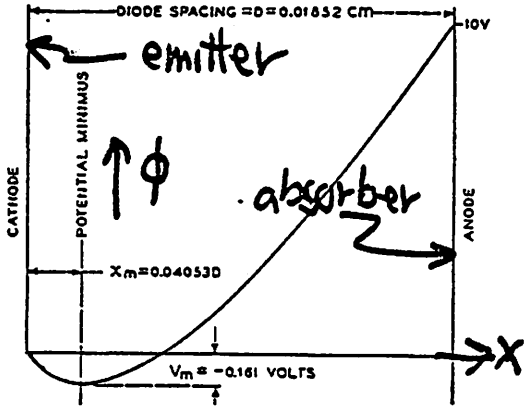

FIG. 1. A schematic sketch of the potential distribution in a space-charge limited diode.

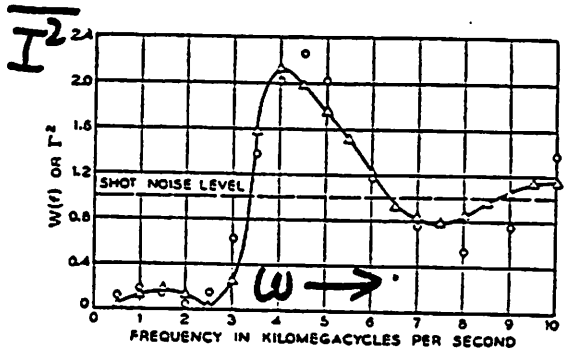

FIG. 7. The frequency spectrum of the current fluctuation.

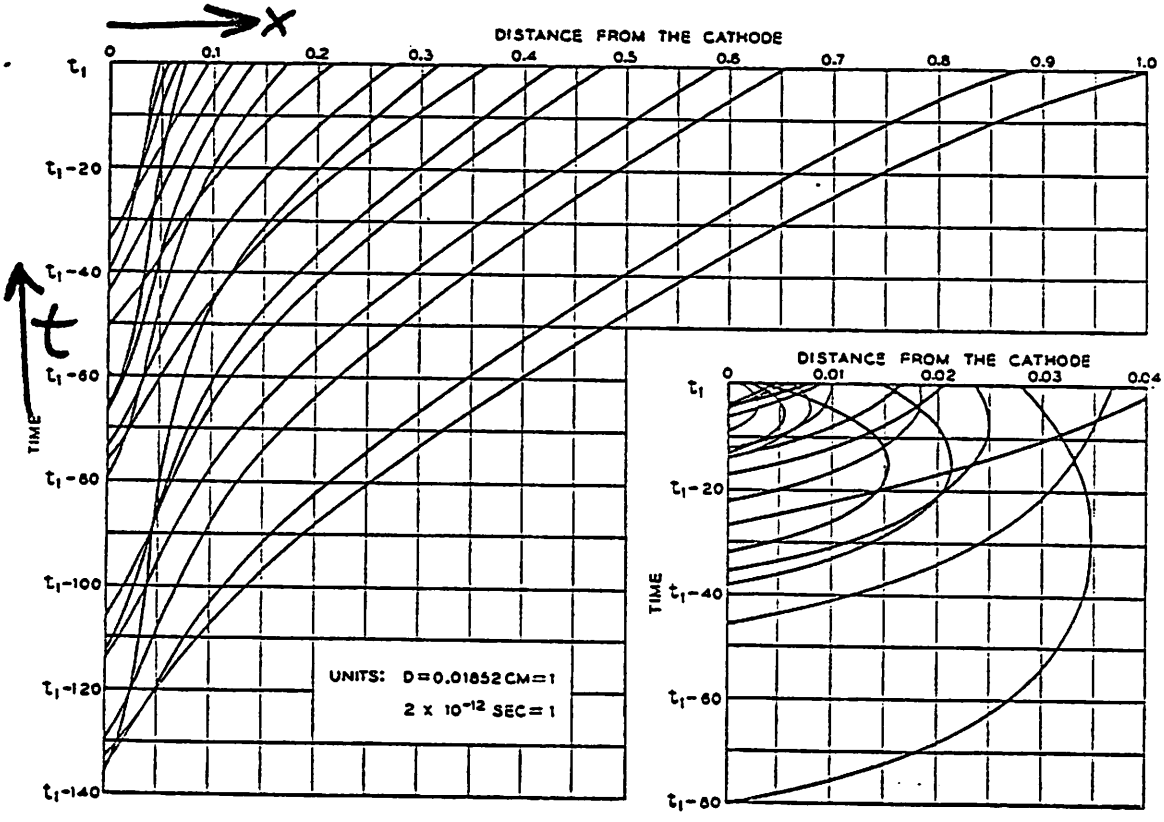

FIG. 4. Some typical electron trajectories.

On average 363 electrons in diode, 165 between emitter and potential minimum

ELECTRON DIODE (ROUSSET, BIRDSALL, 1981)

$t=0$ conditions

$\phi(0) = 0 = \phi(L)$

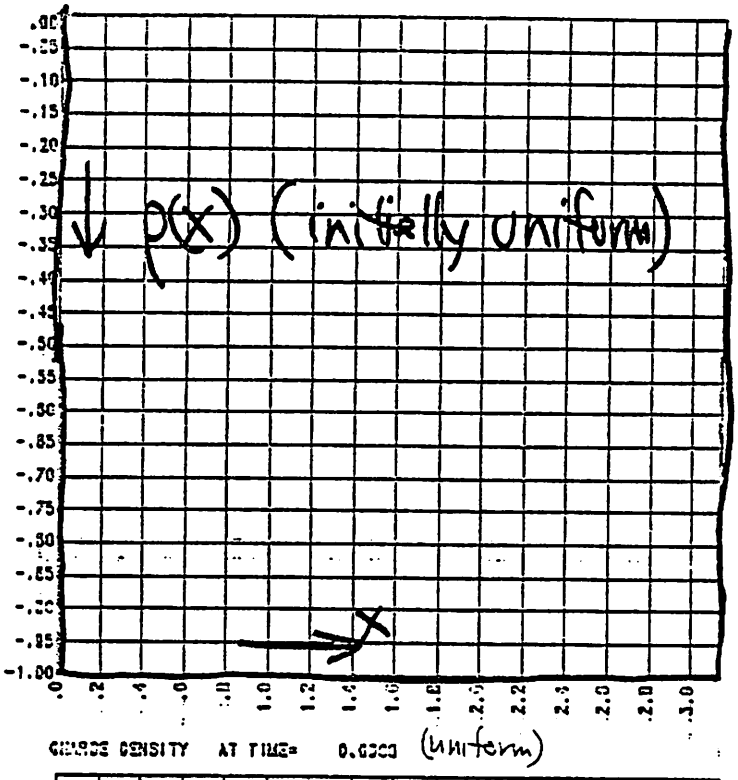

(uniform)

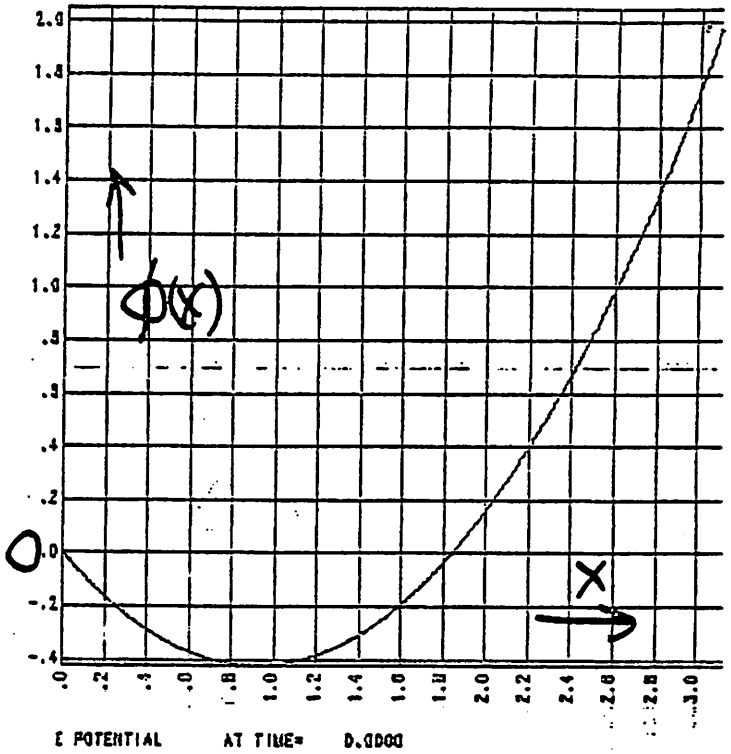

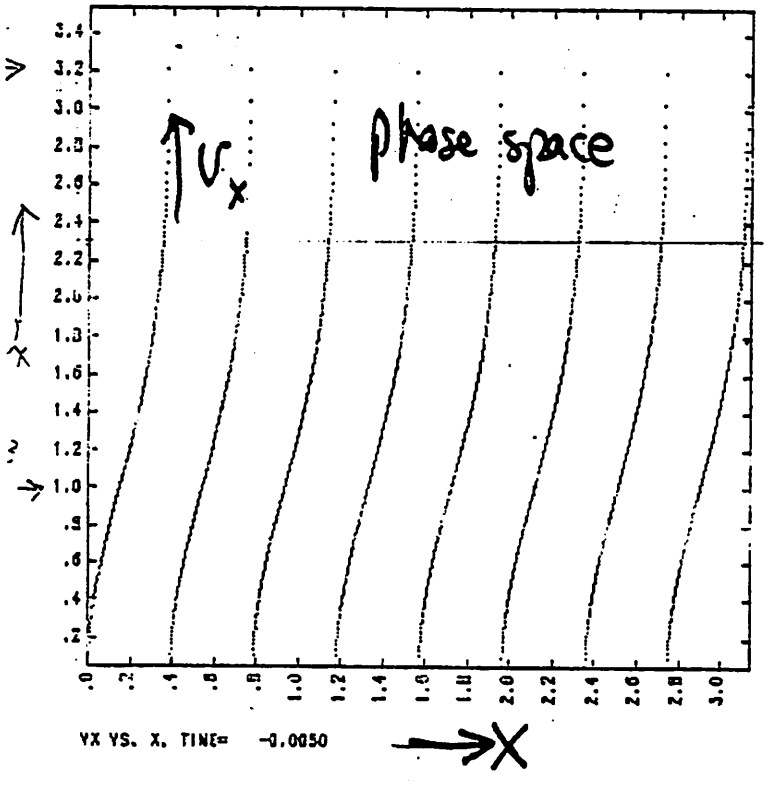

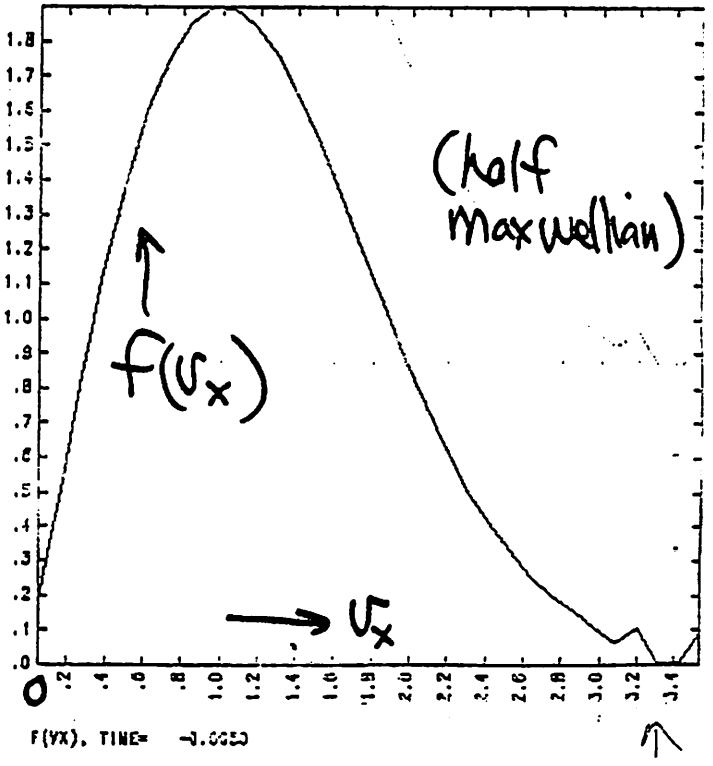

$t = 5.0$

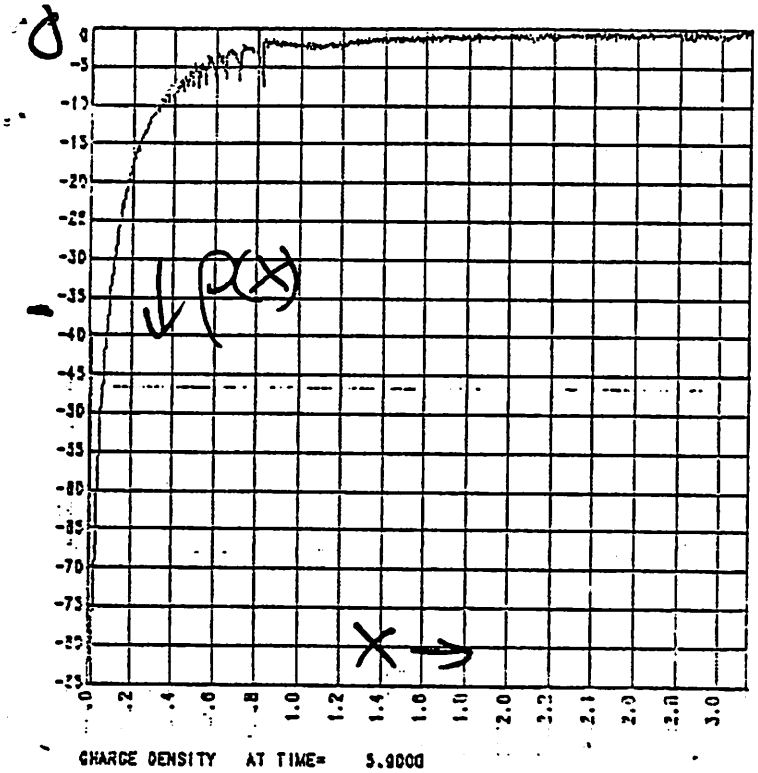
ρ(x)
X
CHARGE DENSITY AT TIME= 5.0000

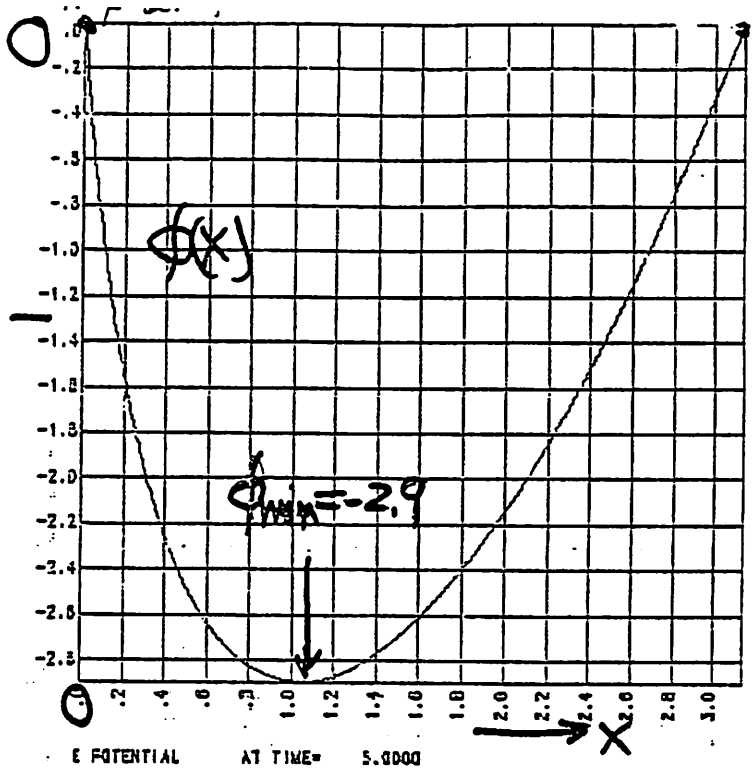
φ(x)
$\varphi_{min} = -2.9$
X
E POTENTIAL AT TIME= 5.0000

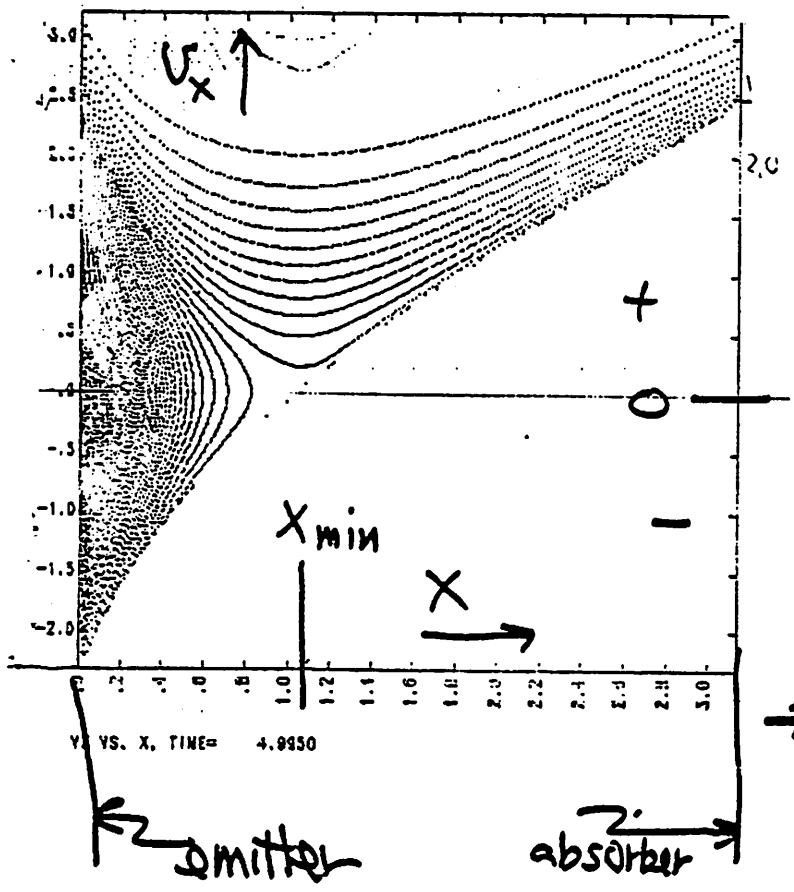
v_x
+
0
−
X_{min}
X
emitter
absorber

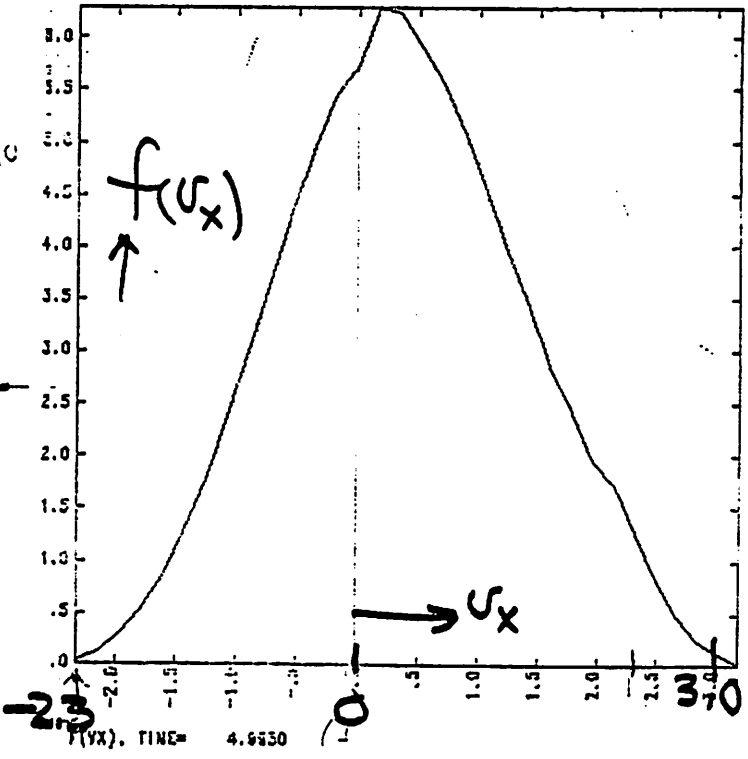
$f(v_x)$
v_x
-2.3
0
3.0

time histories

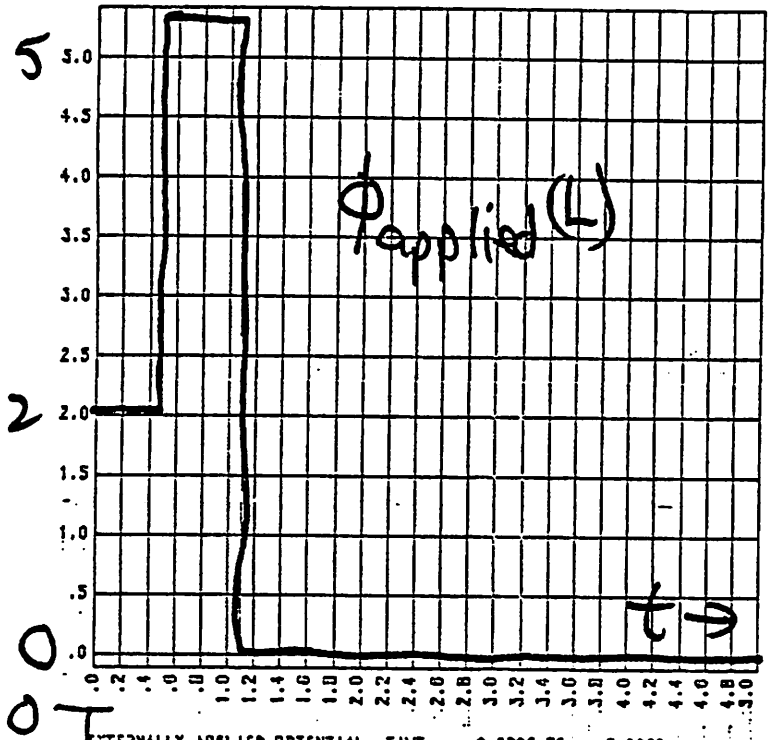

EXTERNALLY APPLIED POTENTIAL, TIME= 0.0000 TO 5.0000

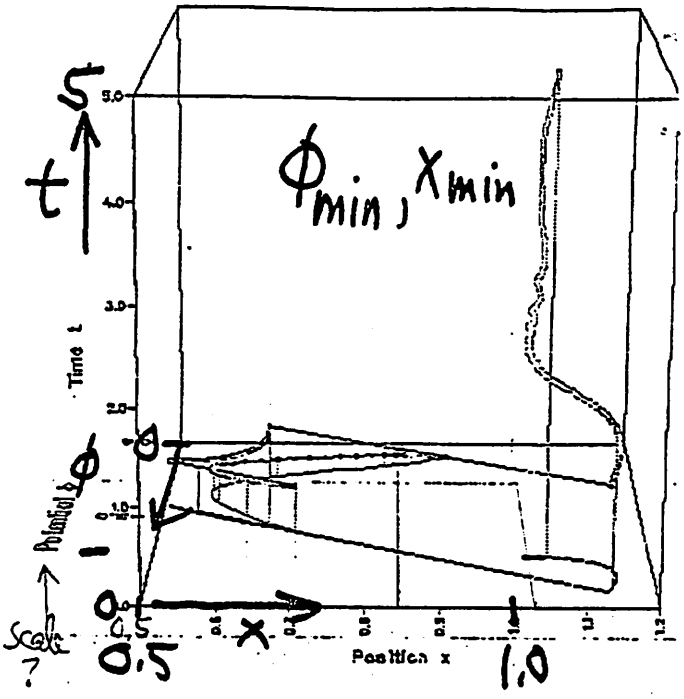

POTENTIAL MINIMUM, TIME= 0.0000 TO 5.0000

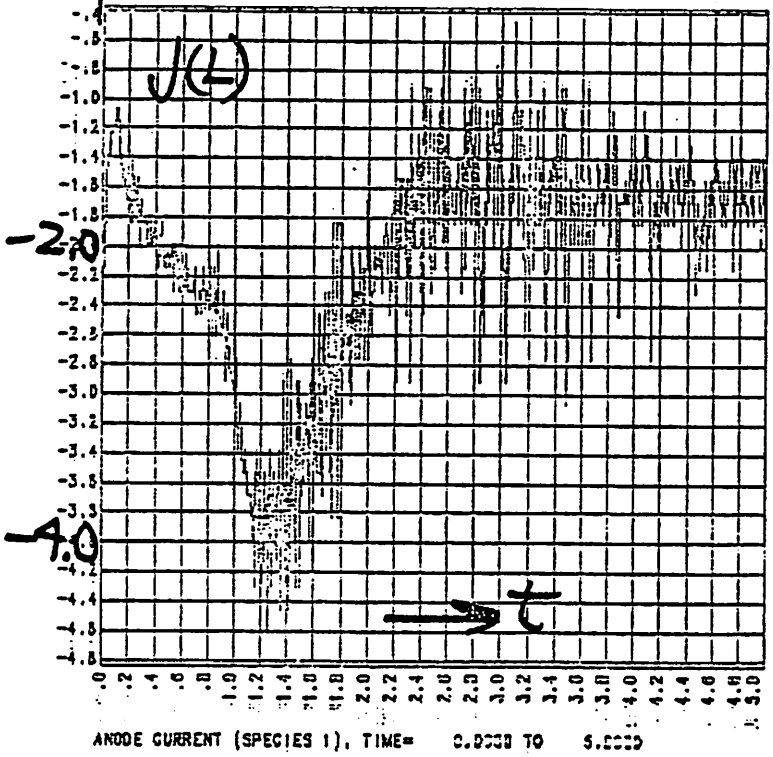

ANODE CURRENT (SPECIES 1), TIME= 0.0000 TO 5.0000

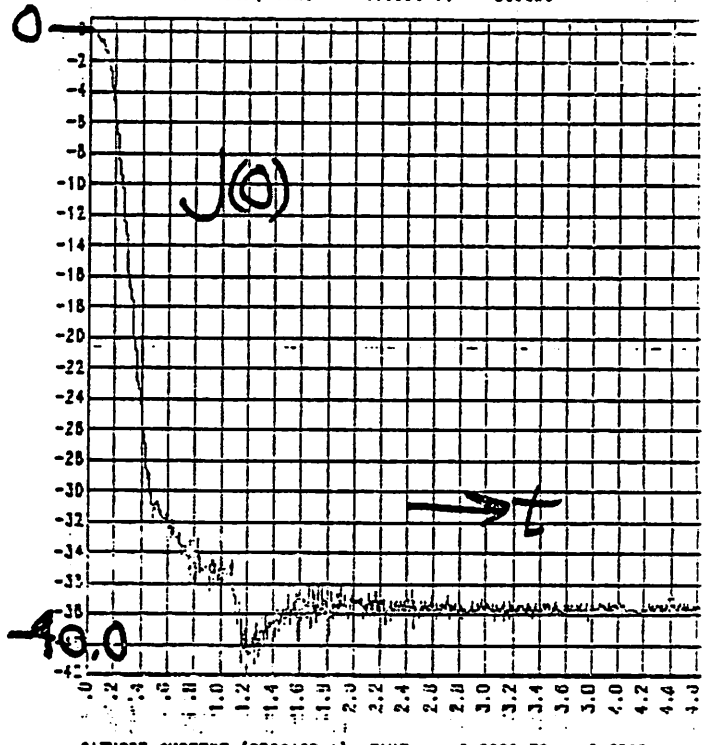

CATHODE CURRENT (SPECIES 1), TIME= 0.0000 TO 5.0000

time histories

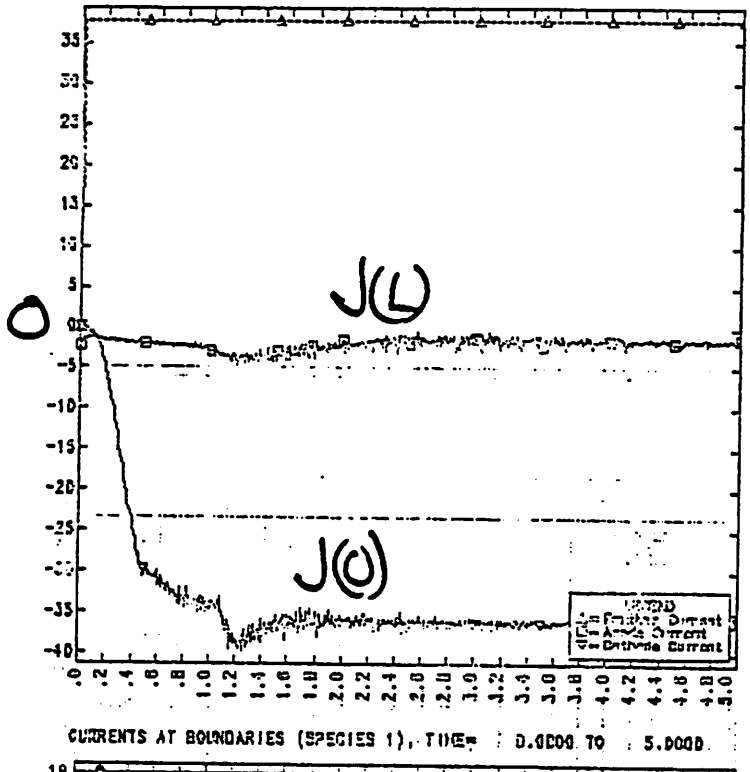

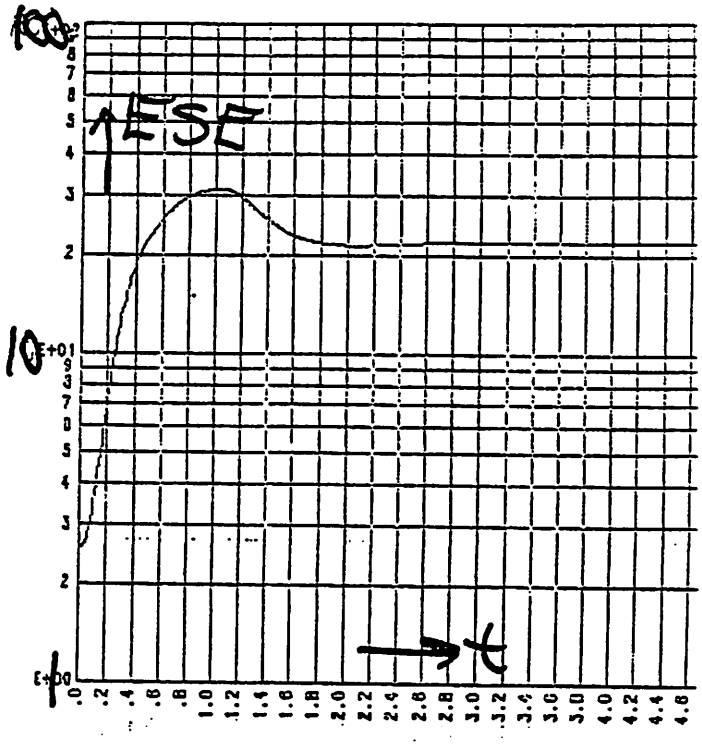

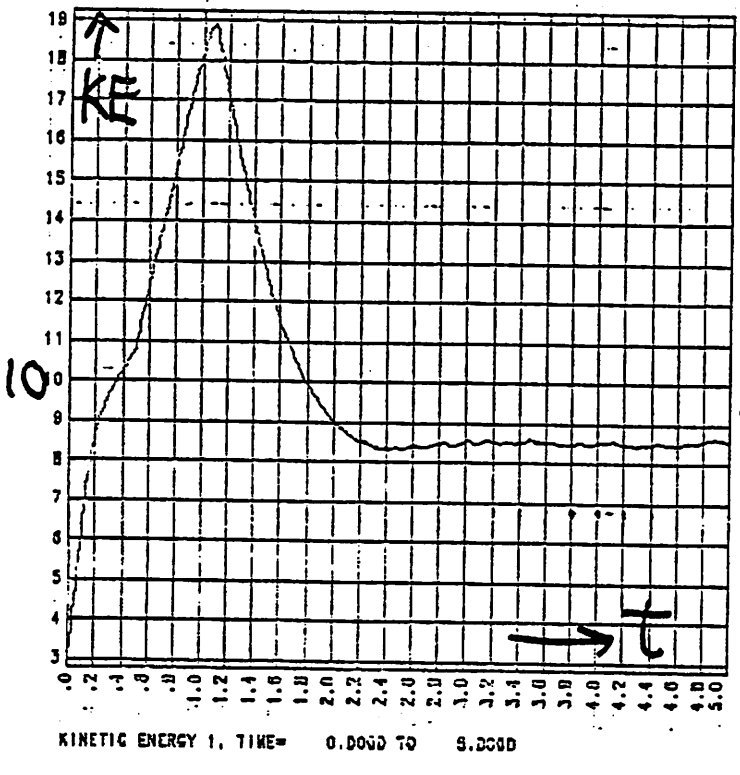

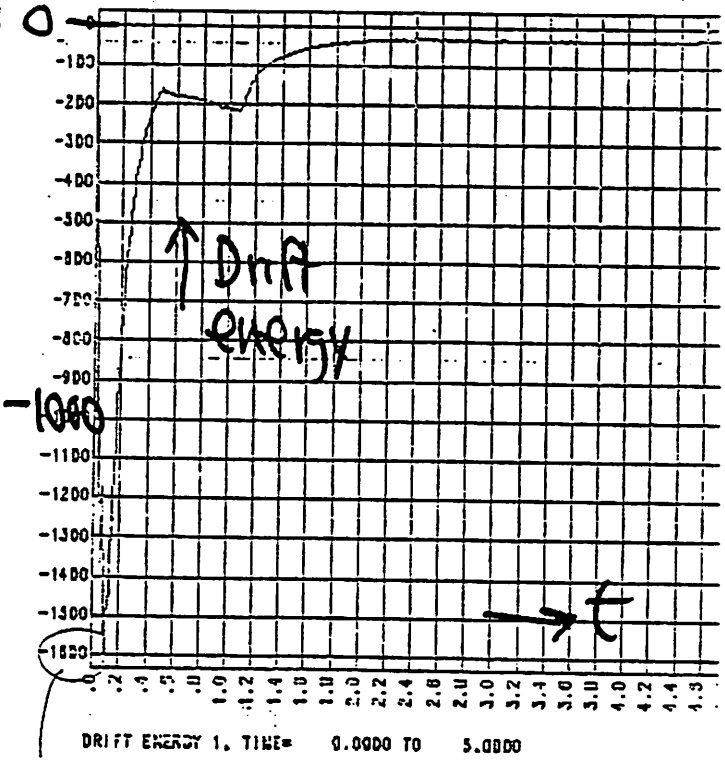

time histories

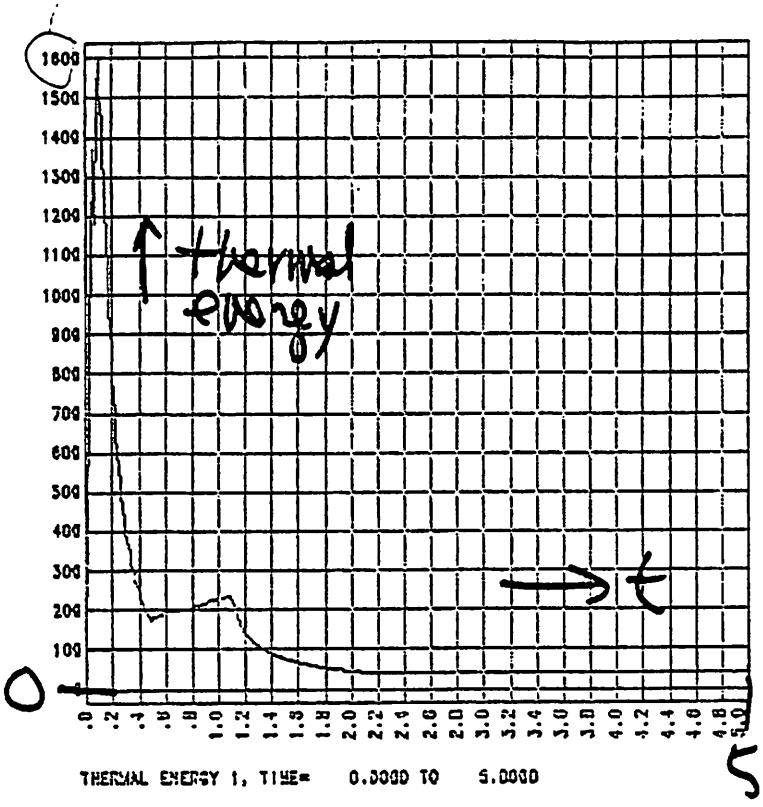

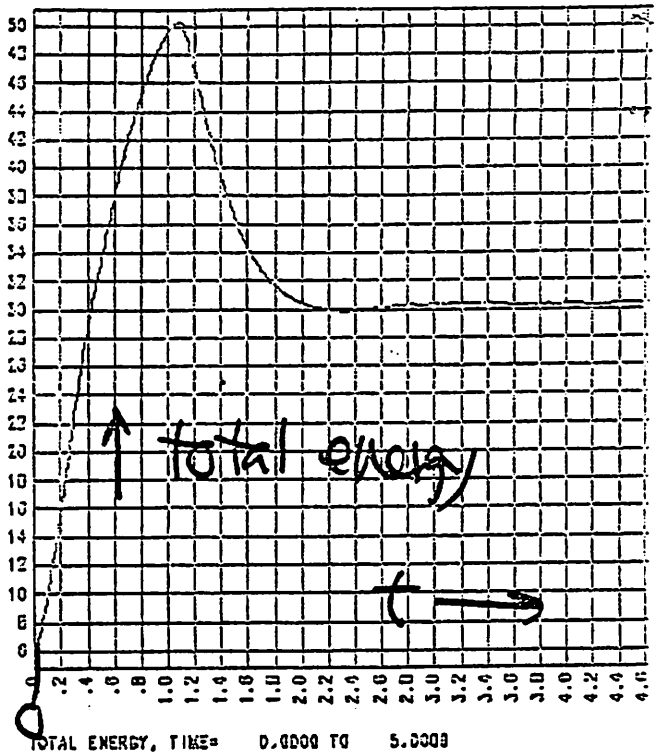

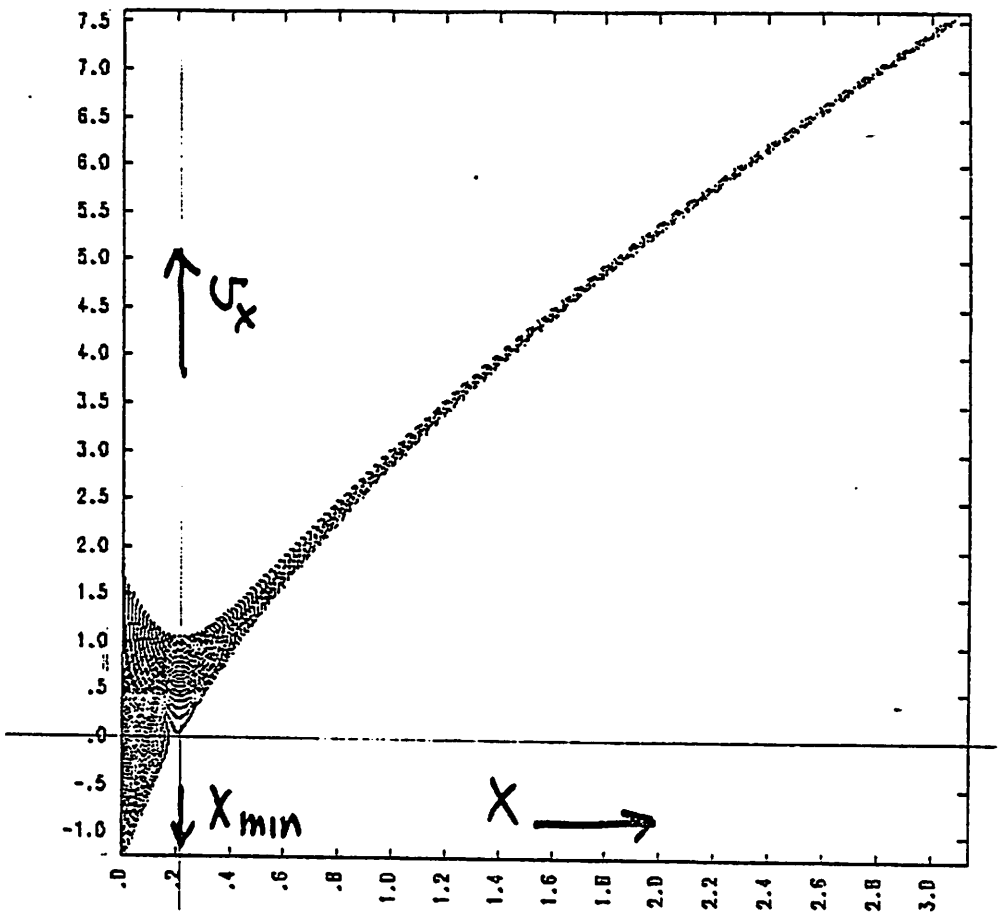

VX VS. X, TIME= 9.9950

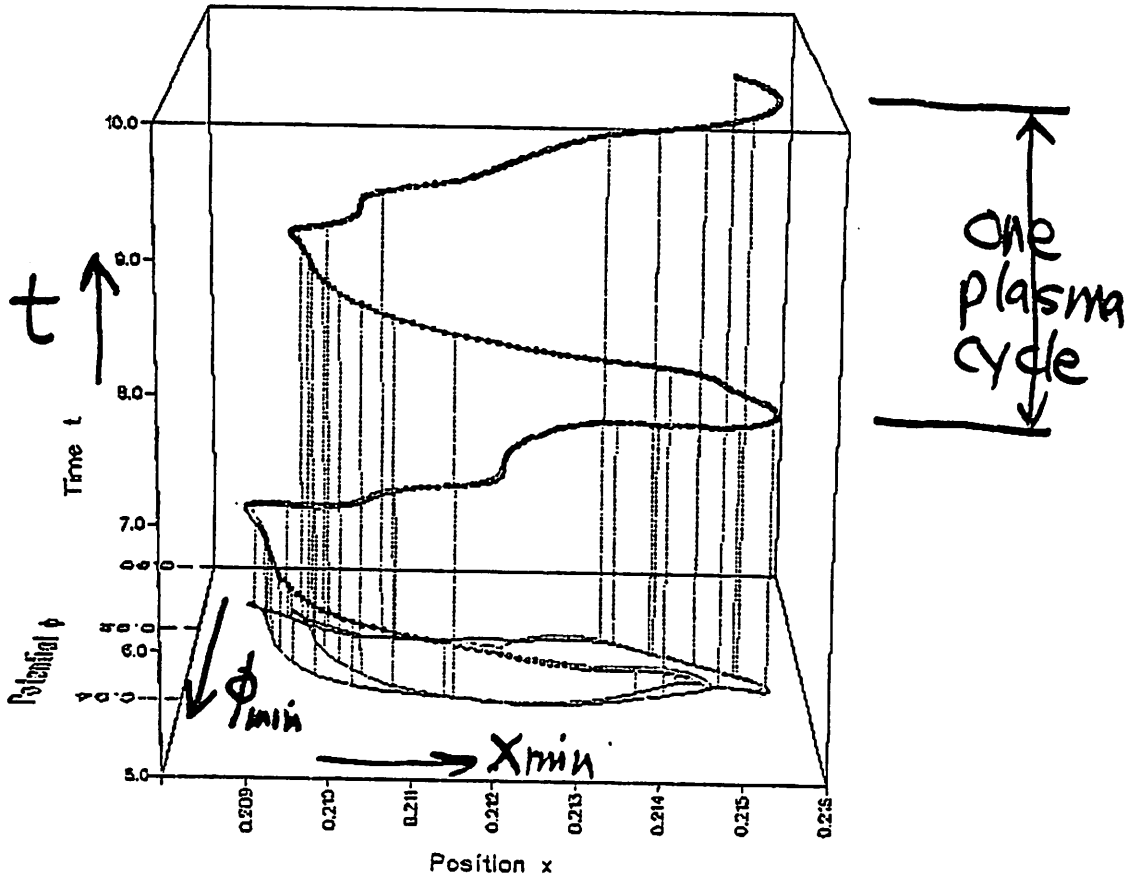

POTENTIAL MINIMUM, TIME= 5.0000 TO 10.0000

ELECTRON DIODE, Beam injected

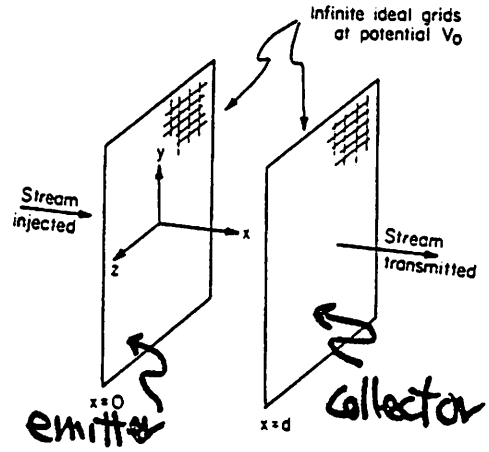

FIG. 3.01a. Stream and electrode configuration for the classical infinite-stream model.

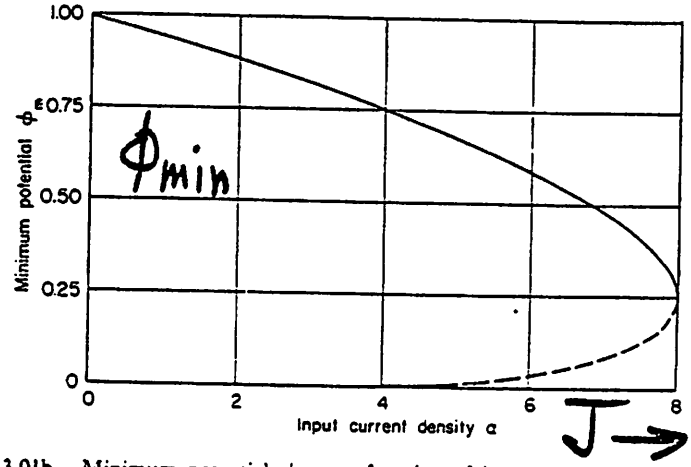

FIG. 3.01b. Minimum potential ϕ_m as a function of input current α. The dotted portion is called the "C-overlap" solution and is excluded by stability considerations.

Birdsall & Bridges (1961, 1963, 1966)

time-independent solutions

(a)

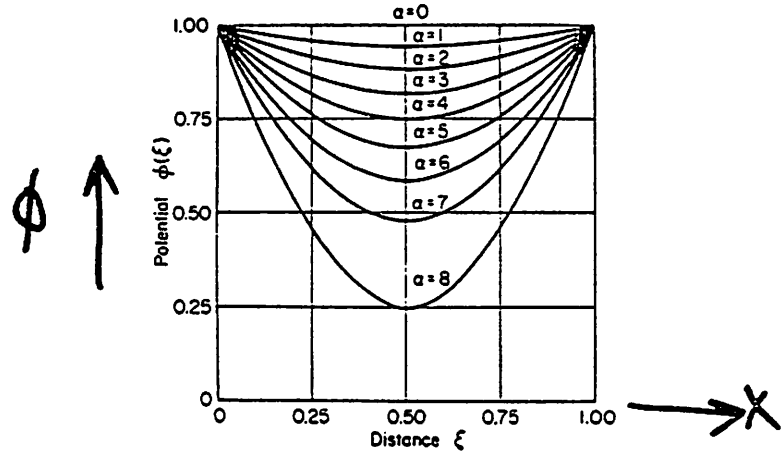

FIG. 3.01c. Potential profiles in the interelectrode space for the classical, positive potential-minimum solutions with input currents between 0 and 8.

(b)

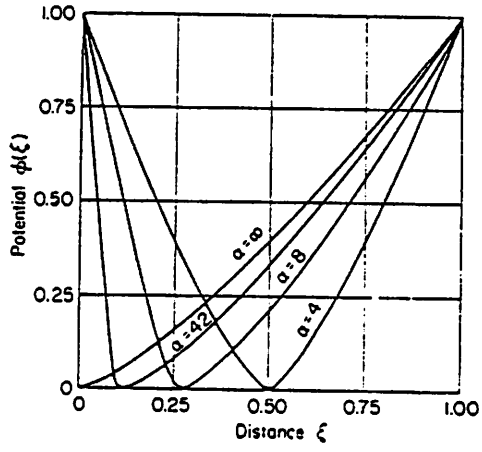

Virtual cathode solutions

FIG. 3.01d. Potential profiles in the interelectrode space for the classical virtual-cathode solutions with input currents between 4 and ∞.

$$\alpha \equiv \frac{J}{J_{child-Langmuir}}$$

Time dependent solutions

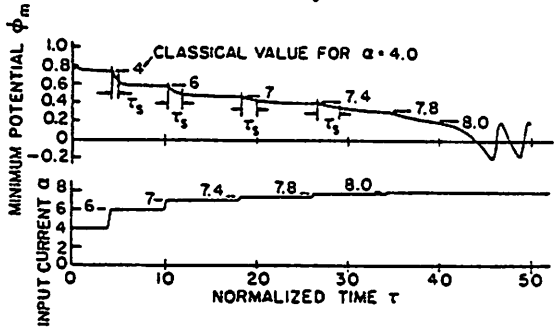

time history of potential minimum

FIG. 3.10a. Time behavior of the potential minimum with increasing input current α.

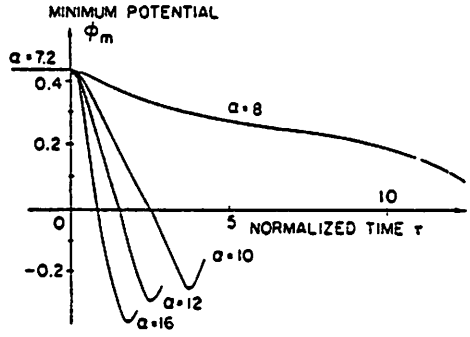

FIG. 3.11b. Decay of the potential minimum from the stable state with $\alpha = 7.2$ when α is increased suddenly to 8, 10, 12, or 16.

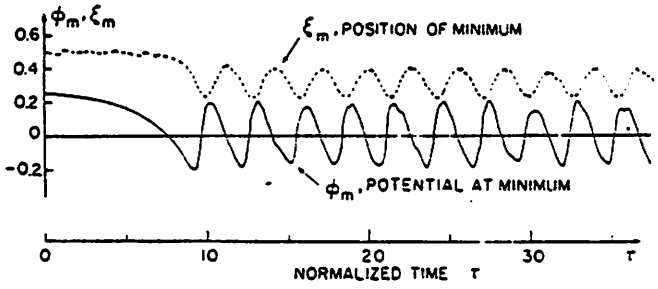

FIG. 3.11a. Time behavior of the potential minimum (minimum potential ϕ_m, position ξ_m) with $\alpha = 8$, showing decay from the stable mode with $\alpha = 8$.

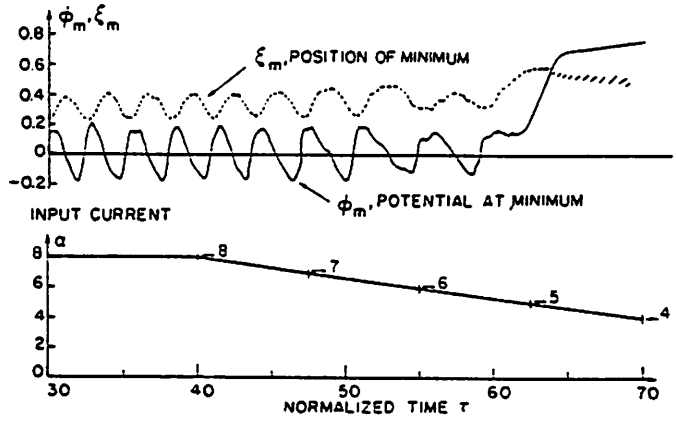

FIG. 3.11f. Continuation of Fig. 3.11a, but with decreasing injected current. The recovery of the stable state occurs around $\alpha = 5$, sooner than in the classical analysis. The sawtooth shape of ξ_m is caused by the computer program's shift in selection between two sheets at almost the same potential.

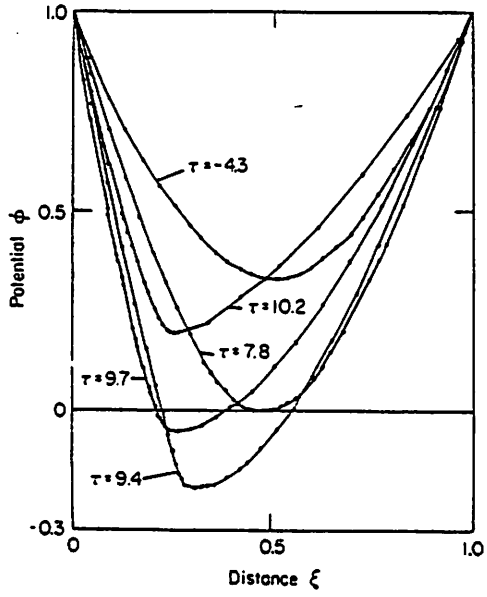

FIG. 3.11c. Potential profiles in the space at times $\tau = -4.3$, 7.8, 9.4, 9.7, and 10.2. The dots show the potentials at the positions of all the sheets used; straight lines join the dots.

details of oscillating potential minimum

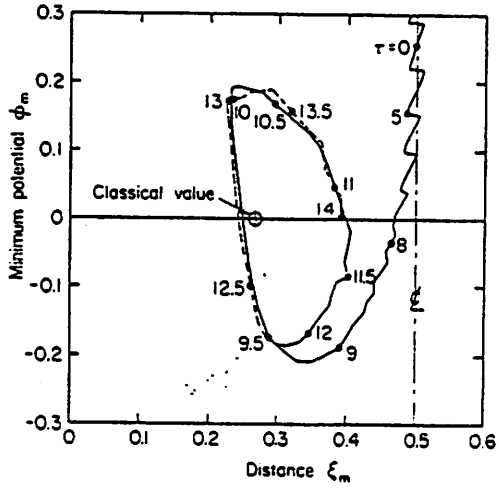

FIG. 3.11d. Locus of the minimum ϕ_m in the space. Time τ is given at points along the curve. The sawtooth shape of the curve from $\tau = 0$ to $\tau = 8$ is caused by the computer program's shift in selection between two sheets that are at almost the same potential. The point labeled "classical value" is that given by the analysis of Section 3.01.

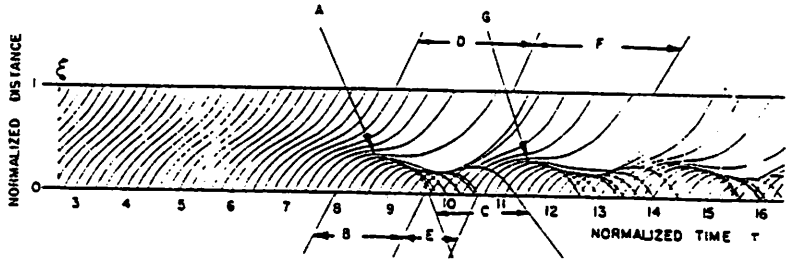

FIG. 3.11e. Trajectories for part of the time interval of Fig. 3.11a, showing the initial decay and first few cycles of oscillation. For clarity, the trajectory of only every fourth sheet used in the calculation is shown.

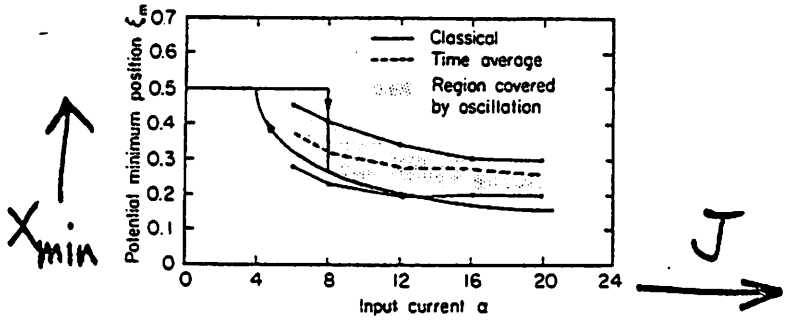

FIG. 3.11h. Potential minimum position ξ_m as a function of α for both classical and dynamic analyses.

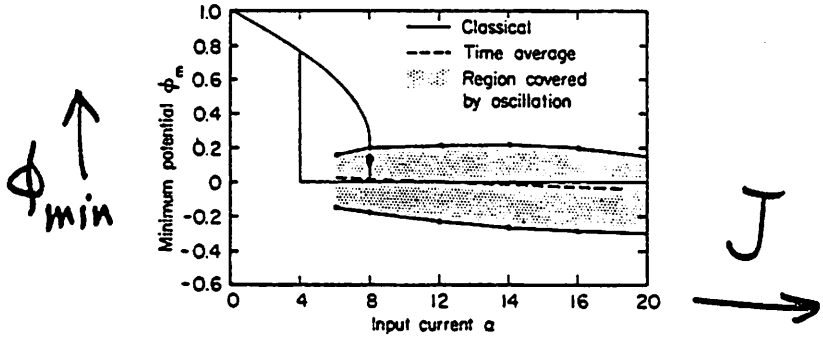

FIG. 3.11i. Minimum potential ϕ_m as a function of α for both classical and dynamic analyses.

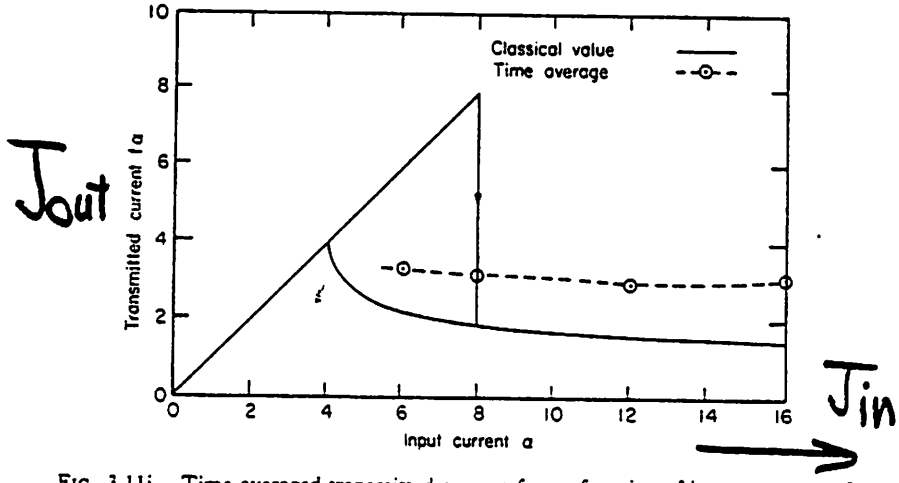

FIG. 3.11j. Time-averaged transmitted current $f\alpha$ as a function of input current α for both classical and dynamic analyses.

Differences between time independent solutions and average of time-dependent solutions.

DIODE ENERGIES

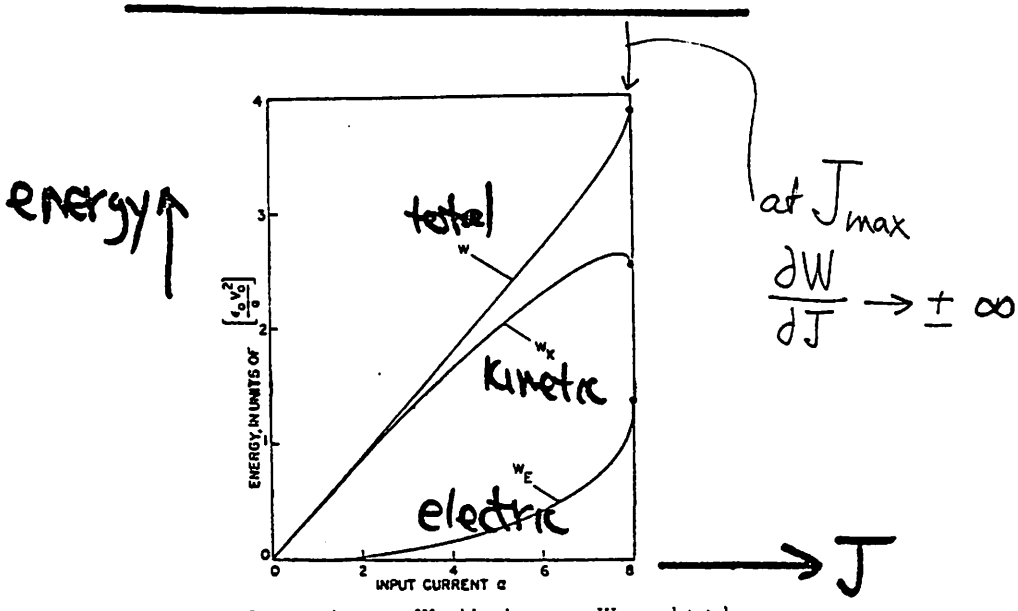

FIG. 22. Computed energy W_E, kinetic energy W_K, and total energy $W = W_E + W_K$ in the interelectrode space as a function of input current.

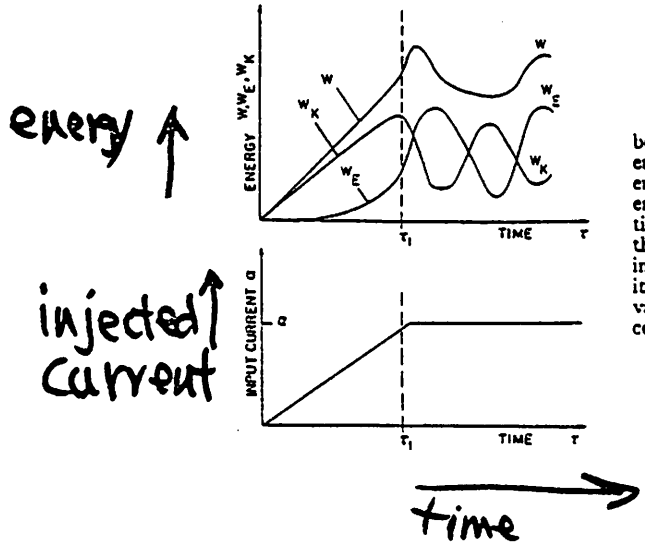

FIG. 23. Expected behavior of total energy W, electric energy W_E, and kinetic energy W_K as functions of time when the input current is increased slowly past its maximum stable value and then held constant.

FINITE DIAMETER BEAM

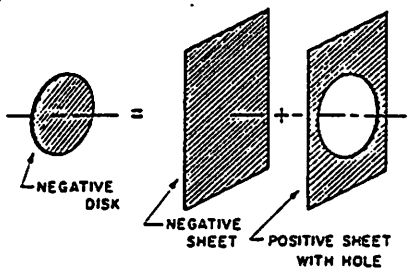

FIG. 16. Schematic representation of a disk charge as the superposition of an infinite sheet charge and an infinite sheet of opposite sign with a hole.

model
(disk diameter = 2b, diode length = a)

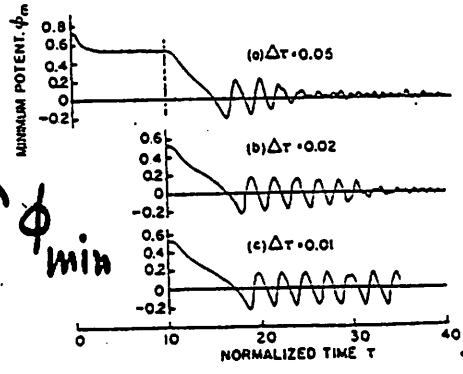

b/a = 0.63

ϕ_{min}

t

instability initiation

FIG. 17. Time history of the potential minimum for a cylindrical stream with $b/a = 0.636$. Between $\tau = 0$ and $\tau = 10$ the input current α was 8 and a stable potential minimum occurred. From $\tau = 10$ to $\tau = 11$ the injected current was increased linearly from $\alpha = 8$ to $\alpha = 12$, and the stream goes into the oscillatory state. $\tau_{limiting} = 11.2$. The same run was repeated with computer integration times of (a) $\Delta\tau = 0.05$, (b) $\Delta\tau = 0.02$, (c) $\Delta\tau = 0.01$ to show the effect of errors.

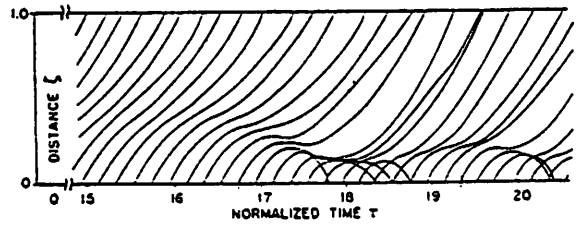

b/a = 0.127

trajectories;
70% transmitted
(40% for sheets,
20% time independent)

FIG. 19. Trajectories for $b/a = 0.127$ showing the large acceleration in the region of the potential minimum and the small accelerations outside this region.

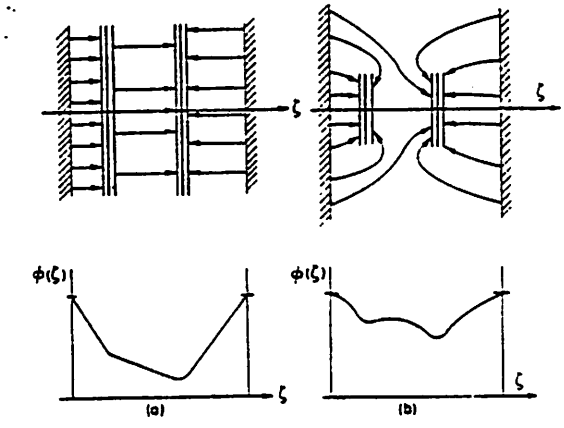

model to show possibility of two minima with cylindrical beam (observed in simulations)

FIG. 18. Schematic representation of the potential profiles in the interelectrode space for two bunches of charges when they are (a) infinite sheets and (b) disks.

ELECTRON AND ION DIODE, Warm emitter

JOURNAL OF APPLIED PHYSICS VOLUME 30, NUMBER 2 FEBRUARY, 1959

Space Charge Neutralization by Positive Ions in Diodes

P. L. Auer and H. Hurwitz, Jr.
General Electric Research Laboratory, Schenectady, New York
(Received June 27, 1958)

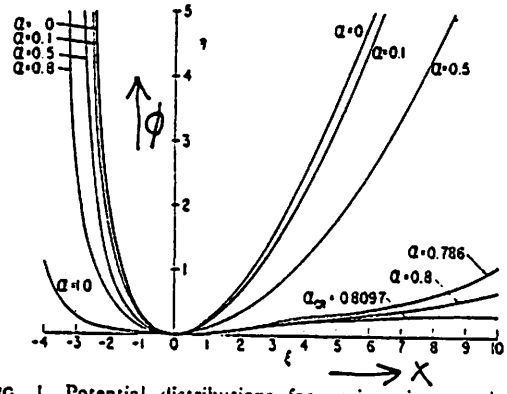

FIG. 1. Potential distributions for various ion to electron density ratios. Reduced variables given by Eqs. (2) and (4).

$$\alpha \equiv \left.\frac{n_i}{n_e}\right|_{\text{potential minimum}}$$

Anomalous behavior $0.81 < \alpha < 1.0 \rightarrow$

($\alpha = 0$ is Langmuir electron diode)

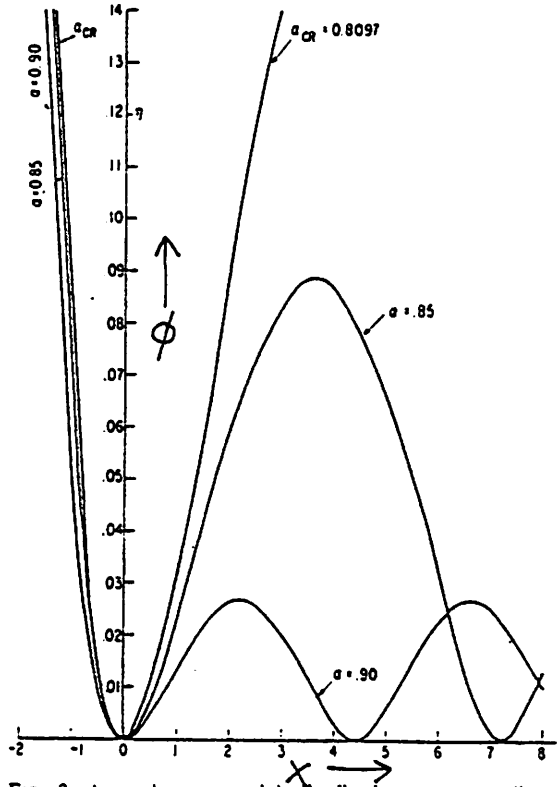

FIG. 2. Anomalous potential distributions corresponding to $\alpha \geq \alpha_{CR}$. Note the disparity in scale between this figure and the previous one.

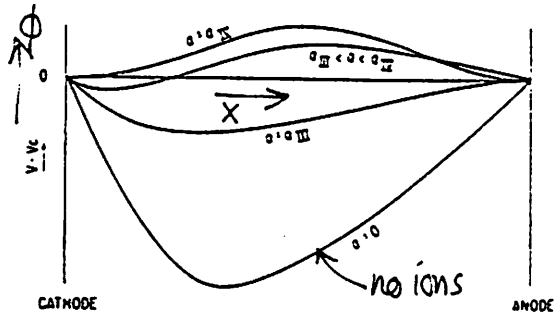

FIG. 3. Schematic evolution of potential distribution with increasing ion density for diode at constant saturation current, with fixed length and zero anode to cathode voltage drop.

Also obtained two possible solutions with $\alpha > \alpha_{IV}$

Hints at instability

(More on this by P. Burger, 1967)

All time independent.

Special model

$\phi(0) = 0 = \phi(L)$ short circuit

$I_{saturation}$ constant as α increased.

At α_{III} $\begin{cases} E(L) = 0 \\ \phi(x) < 0 \quad \text{all } x \end{cases}$

If L large, $\alpha_{III} > \alpha_{CRITICAL}$

At $\alpha > \alpha_{III}$ pot. min and pot. max

At $\alpha = \alpha_{IV}$ $\begin{cases} \text{no more pot. min} \\ E(0) = 0 = E(L) \\ I = I_{sat.} \end{cases}$

JOURNAL OF APPLIED PHYSICS VOLUME 31, NUMBER 12 DECEMBER, 1960

Potential Distributions in a Low-Pressure Thermionic Converter

PETER L. AUER
General Electric Research Laboratory, Schenectady, New York
(Received August 2, 1960)

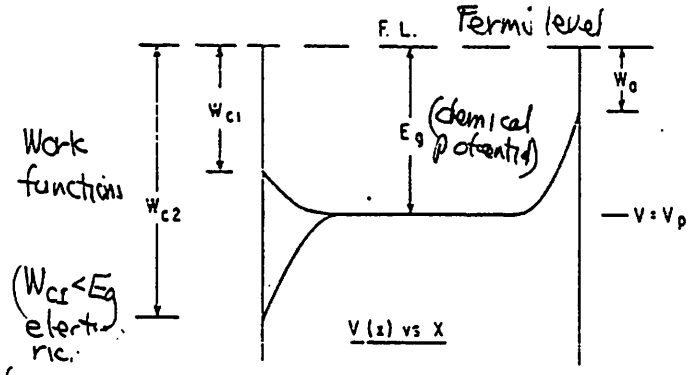

FIG. 1. Potential sheath distributions at thermodynamic equilibrium.

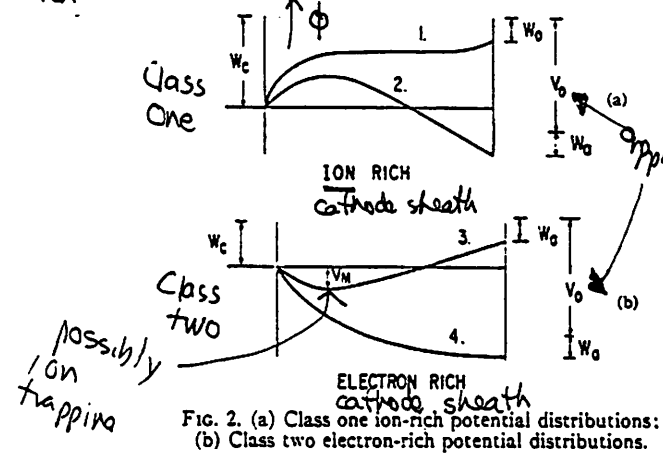

FIG. 2. (a) Class one ion-rich potential distributions; (b) Class two electron-rich potential distributions.

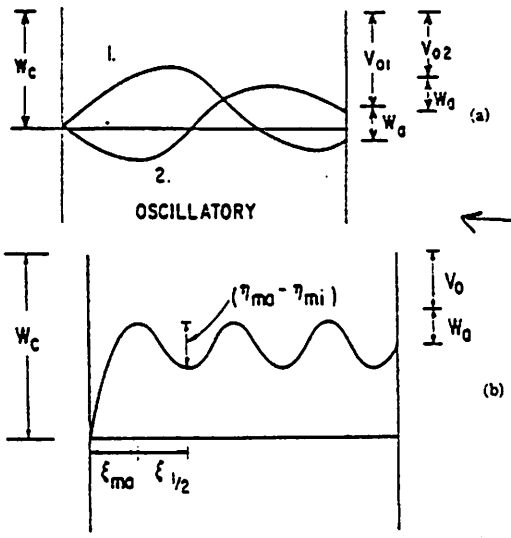

FIG. 3. Class three oscillatory potential distributions.

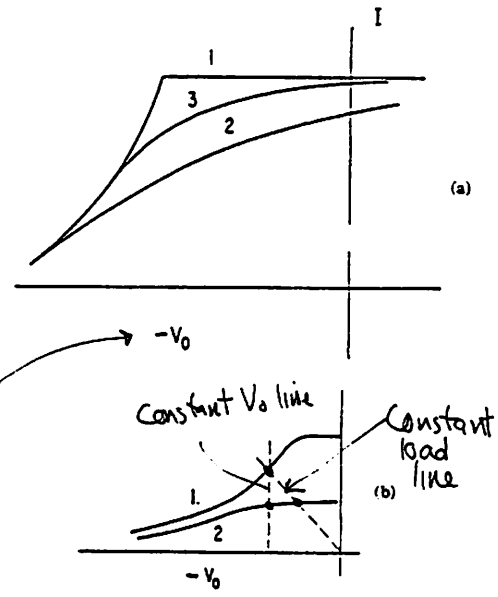

FIG. 4. (a) Current voltage plots corresponding to three classes of potential distributions; (b) Possible bistable mode.

Fermi level

Work functions

$(W_{c1} < E_g$ electr... ric.

$(W_{c2}$ ... ion rich

Class One

ION RICH cathode sheath

Class two

possibly ion trapping

Applied

"Output"

Constant V_0 line

Constant load line

instability guessed

Transition 1. to 2. by increasing V_0 not possible; transition 4. to 3. by decreasing V_0 not possible.

Must pass to class three which contains all oscillatory solutions.

All time independent

$\frac{1}{2}mv^2 + q\phi = \text{constant}$

PLASMA PROPULSION DEVICES

TRANSIENT AND STEADY STATE BEHAVIOR
IN CESIUM ION BEAMS[1]

J. M. Sellen Jr.[2] and H. Shelton[3]

Research Laboratory[4]
Ramo-Wooldridge
Canoga Park, California

Electrostatic Propulsion

Edited by

David B. Langmuir
Space Technology Laboratories, Inc., Canoga Park, California

Ernst Stuhlinger
NASA George C. Marshall Space Flight Center, Huntsville, Alabama

J. M. Sellen, Jr.
Space Technology Laboratories, Inc., Canoga Park, California

ACADEMIC PRESS · NEW YORK · LONDON · 1961

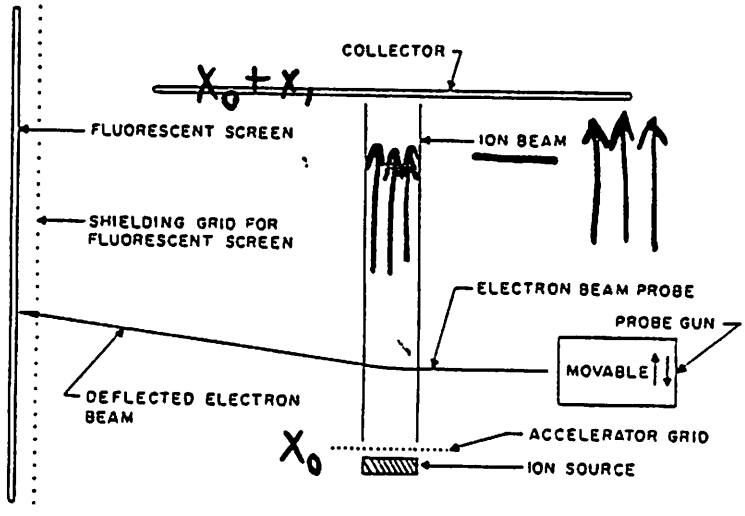

Fig. 22. A sketch of the electron beam probe being directed through the ion beam.

There is neutralization by electrons.

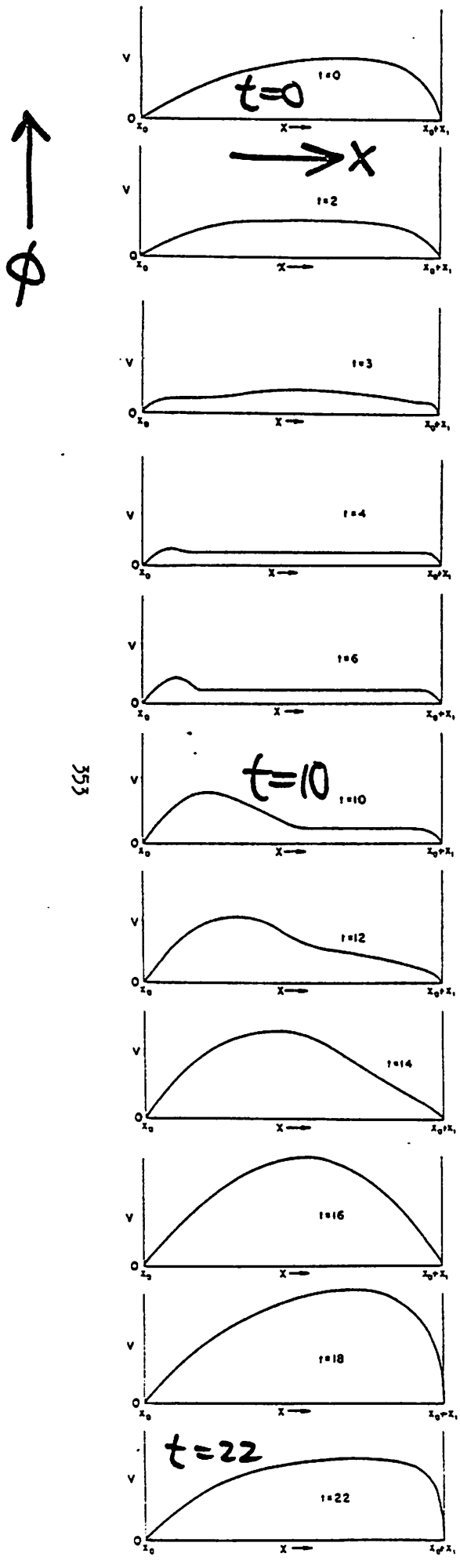

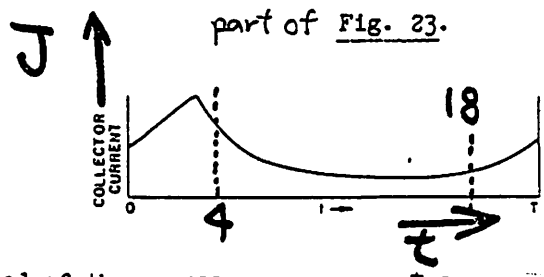

The period of the oscillation, T, is ~ 8.5 μsec. The ion acceleration voltage was 200 volts. The collector current through one period of the oscillation is shown in the trace above. The sweep in the probing beam trace and in the collector current trace were triggered simultaneously.

Oscillatory behavior

$f_{osc} \sim \sqrt{V_0}/X_1$, 1/transit time.

Fig. 24.

Δt ~ 0.37 μsec.

Qualitative potential distributions in the grid to collector region obtained from the probing beam data shown in Fig. 23. The time indicated on each trace is the time after t = 0 in the collector current waveform of Fig. 23. The total period there has been rather arbitrarily divided into ~ 23 units. At t = 4units the collector current has already attained its peak and is beginning to decline; at t ~ 18 units the collector current is beginning, once again, to rise to its peak.

Appears like packet (bunch) of ions moving along beam, initiated by perturbation at injection.

Electrons are trapped in beam by ion space charge. Energy spread of ions increased by oscillations.

Computer Experiments on Ion-Beam Neutralization with Initially Cold Electrons

D. A. DUNN* AND I. T. HO†
Stanford University, Stanford, Calif.

Trajectories of electrons and ions shot into an initially field-free space, as in the ion-propulsion problem, have been obtained using a one-dimensional model. The results of a set of computer experiments are presented, in which the ratios of electron-to-ion injection velocities and currents are varied for large but finite ratios of ion-to-electron mass. For electron-to-ion velocity ratios less than about 2, static theories of neutralization are confirmed. For unneutralized and partially neutralized beams, oscillations, and in some cases, randomization of electron trajectories are observed. For electron-to-ion velocity ratios greater than 2 and electron-to-ion current ratios greater than a critical value, neutralization is obtained by means of an oscillating electron sheath that feeds electron current to the ion beam in a self-compensating manner.

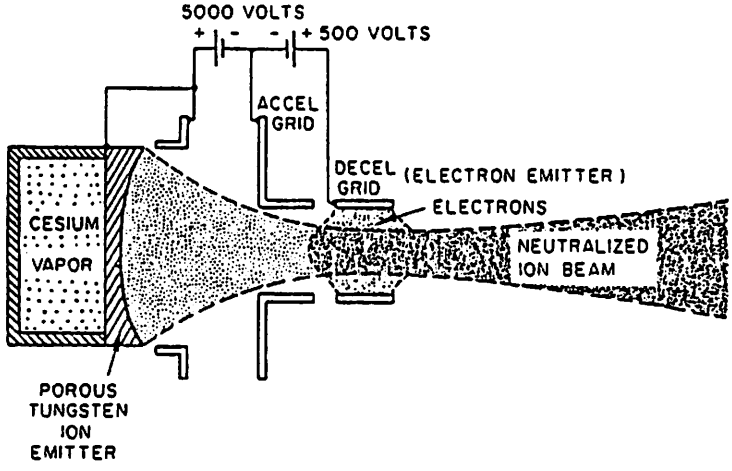

Fig. 6.7-1. Cross-section view of an ion propulsion system.

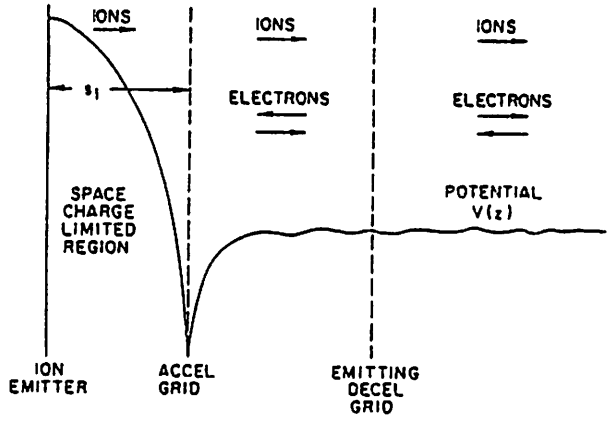

Fig. 6.7-2. A planar ion propulsion system and the associated potential diagram. Such a system would perform about the same as the system of Fig. 6.7-1, except that the grids would be worn down by ion sputtering and limit the life of the system.

Model of Dunn & Ho, cold injection

$$\gamma_0 = \frac{u_{e0}}{u_{i0}}$$

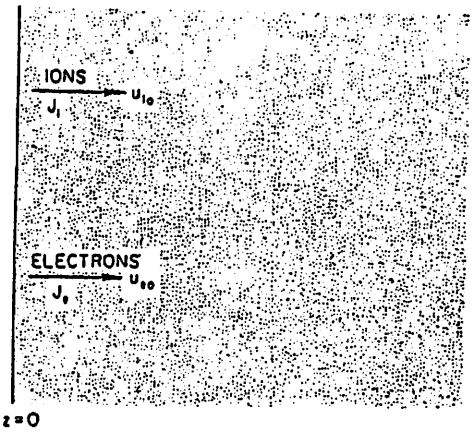

Fig. 6.7-3. One-dimensional model analyzed here has single velocity ion and electron beams injected at $z = 0$.

The injected currents are J_i and J_e and the injection velocities are u_{i0} and u_{e0}. The masses per particle per unit area are m_i and m_e. The injection plane has the property that it is transparent to electrons and ions injected in the positive z-direction, but it collects all particles that strike it traveling in the negative z-direction. The electron current density J_e is equal to the space-charge limited current that would be drawn in a diode of spacing s_e at the potential corresponding to u_{e0}. The corresponding ion-diode spacing is s_i, the spacing of the accel grid from the emitter in Fig. 6.7-2.

Single species; all particles return.

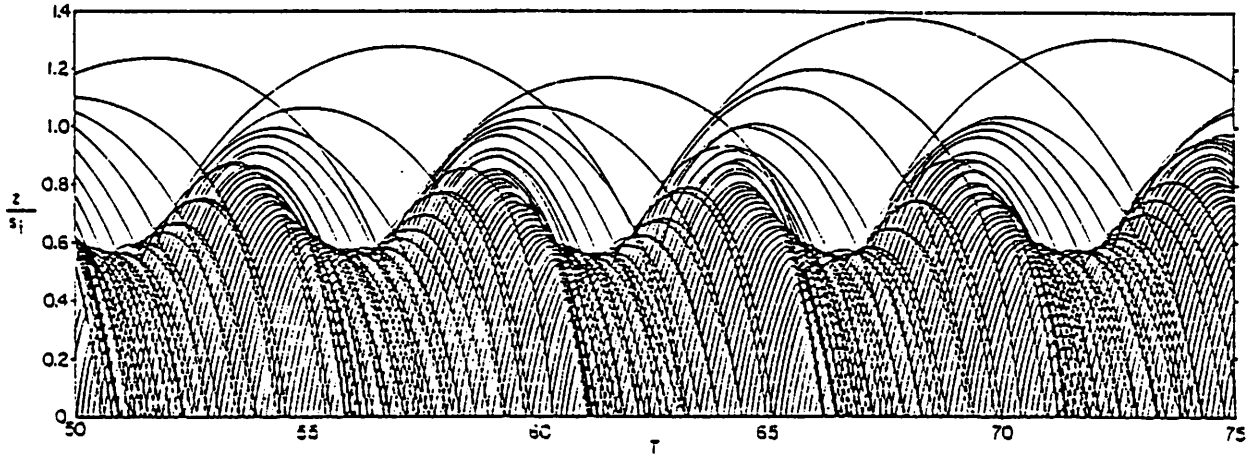

Fig. 6.7-4. Ion trajectories for a single-velocity ion beam injected into an infinite region after an initial transient has died out.

Distance is measured in units of the equivalent space-charge limited diode spacing s_i for the injected current density. Time is measured in ion transit times t_{i0} across the distance s_i at the injection velocity. The pattern repeats except for minor fluctuations due to shot noise. The time step here was $0.25t_0$, rather coarse by modern standards. This computation was done in 1962 with a small computer. For a still coarser time increment by a factor of two the pattern was substantially the same. One ion was introduced per time step [from D. A. Dunn and I. T. Ho, Computer experiments on ion beam neutralization with initially cold electrons, *AIAA J.* 1, 2770–2777 (1963)].

Not static!

$\omega_{oscillation} \approx 2\omega_p$ (at injection plane)

$\approx \omega_p$ (at least penetration plane)

(Also measured experimentally by Sellen and Shelton, 1961

Two species $|J_e| = |J_i|$ at injection plane

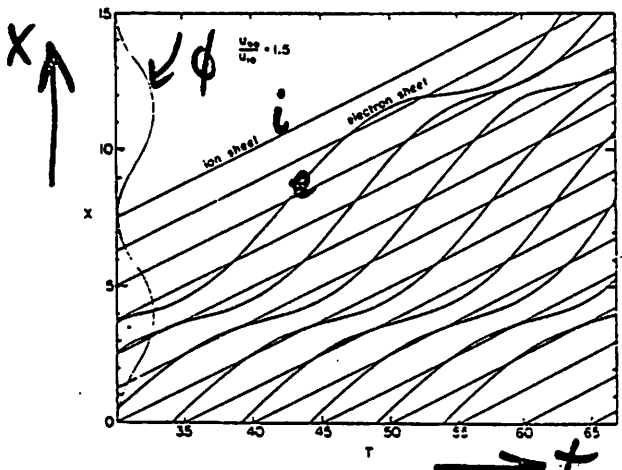

Fig. 9 Trajectories of electrons and ions in a neutralized beam with equal absolute values of injected electron and ion currents for $\gamma_0 = 1.5$ and $(m_i/m_e) = 1800$. Static theory predicts the potential variation at the left and the computed trajectories follow this pattern.

$\gamma_0 = \frac{u_{eo}}{u_{io}} = 1.5$

Agrees with static theory; periodic variation in space, but not in time.

(φ static theory)

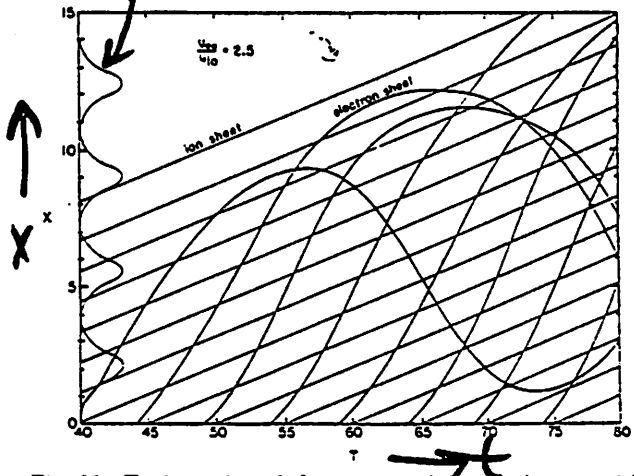

Fig. 10 Trajectories of electrons and ions in beams with injected current neutrality for $\gamma_0 = 2.5$ and $(m_i/m_e) = 1800$. The computed trajectories do not follow the pattern of the static-theory potential variation at the left.

$\gamma_0 = 2.5$

No agreement with static theory; get oscillations in space and in time.

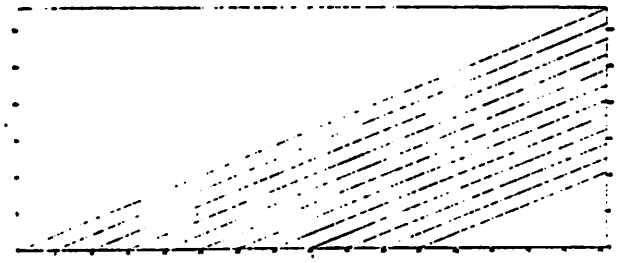

Fig. 11 Ion trajectories for the case of Fig. 10 drawn to a different scale. $\gamma_0 = 2.5$; $(m_i/m_e) = 1800$. Distance X vertically and time T horizontally. Only every fifth trajectory out to $T = 55$ is shown.

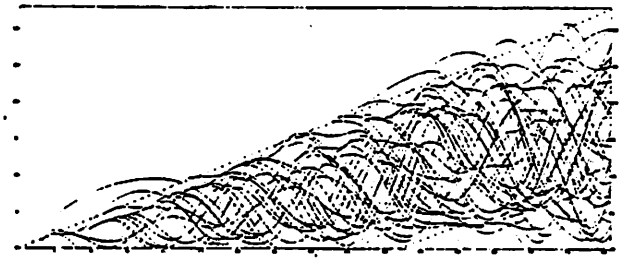

Fig. 12 Electron trajectories that go with the ion trajectories of Fig. 11. $\gamma_0 = 2.5$; $(m_i/m_e) = 1800$. Some electrons return to the injection plane. Distance X vertically and time T horizontally. Ion trajectories for ions injected at $T = 0$ and $T = 52$ are shown as the nearly straight lines with circles.

See next page.

$J_{ef} = |J_i|$,

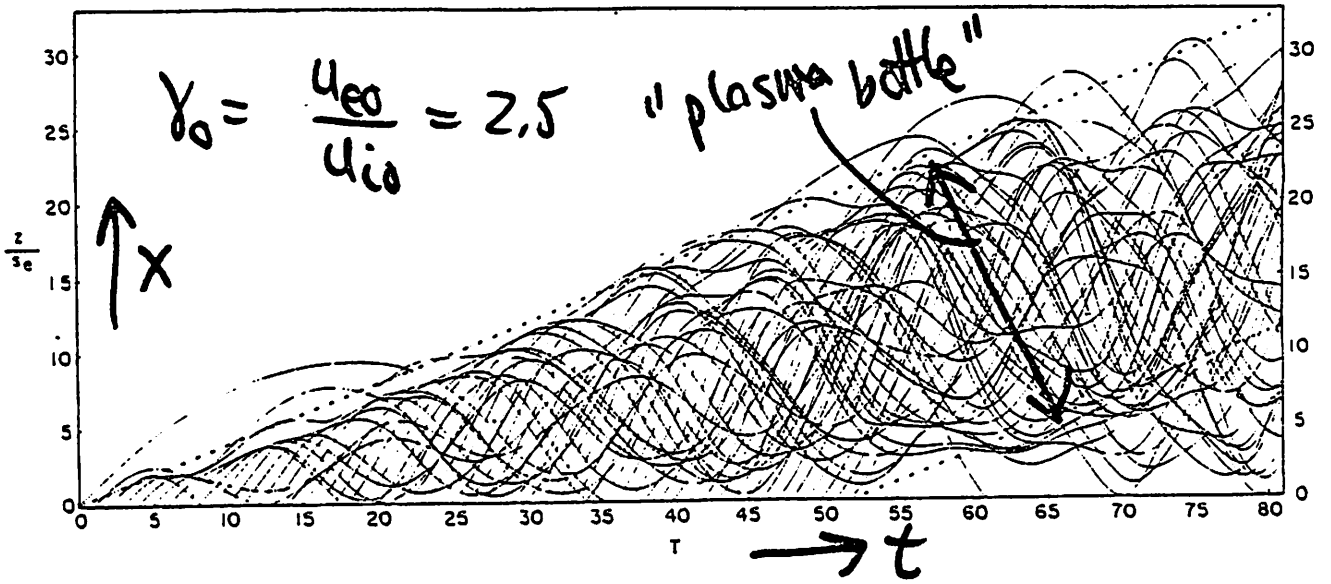

Fig. 6.7-6. Electron trajectories for a two species case with $(u_{e0}/u_{i0}) = 2.5$, $(m_i/m_e) = 1800$, and $(-J_e/J_i) = 1$. The current ratio here is insufficient to give full neutralization and some ions are eventually returned. Only every fifth trajectory out to $T = 55$ is shown, but in the computation electrons were injected uniformly beyond this time. Note that some electrons have already been returned to the injection plane at this time. The trajectory pattern here is the justification for regarding the beam as a "plasma bottle" [from D. A. Dunn and I. T. Ho, Computer experiments on ion beam neutralization with initially cold electrons, *AIAA J.* 1, 2770–2777 (1963)].

Some e are returned to input plane, $x=0$.

Run longer in time, e and i turn back in substantial numbers.

Conclusion: $\gamma_0 \leq 2$ static theory all right

$\gamma_0 \geq 2$ "plasma bottle" " "

$|J_e| > |J_i|$, more electrons injected than ions.

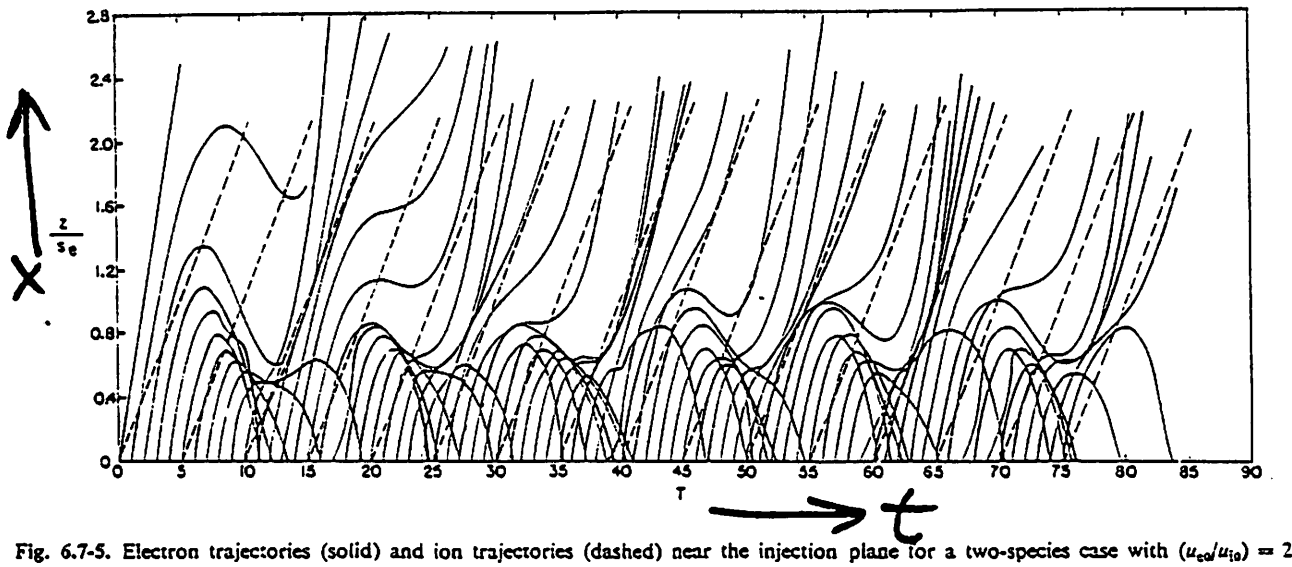

Fig. 6.7-5. Electron trajectories (solid) and ion trajectories (dashed) near the injection plane for a two-species case with $(u_{eo}/u_{io}) = 2.5$, $(m_i/m_e) = 50$, and $(-J_e/J_i) = 2$.

The current ratio for this case is large enough to give complete neutralization by means of an oscillating electron sheath which supplies all the electron current needed for neutralization at velocities randomly distributed about the ion velocity. Distance is measured in units of s_e, the equivalent space-charge limited diode spacing corresponding to the injected electron current. Time is measured in units of the electron transit time t_{eo} across s_e [from D. A. Dunn and I. T. Ho, Computer experiments on ion beam neutralization with initially cold electrons, *AIAA J.* 1, 2770–2777 (1963)].

$|J_e| = 2|J_i|$, $\gamma_0 = \frac{u_{eo}}{u_{io}} = 2.5$

Oscillating electron sheath near emitting plane supplies e's for neutralization. Potential minimum just as with e alone, oscillating in t and x. Minimum acts as virtual electron emitter. Beyond minimum, $|J_e| \cong |J_i|$

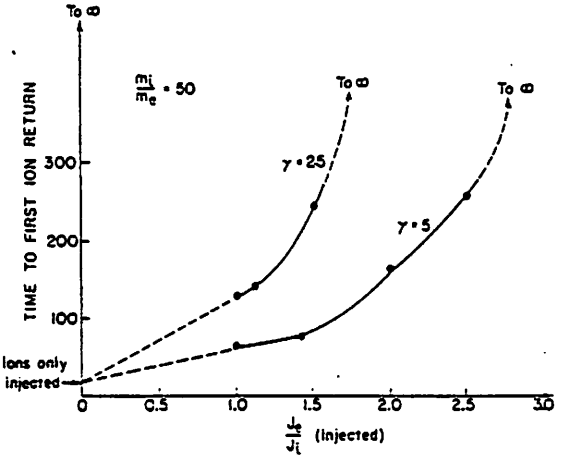

Fig. 14 Time to first ion return as a function of the ratio of injected electron current to ion current, for $\gamma_0 = 2.5$ and $(m_i/m_e) = 50$. When this current ratio is increased, the ions stay in the system longer. If the current ratio is increased far enough, the ions do not return at all.

SUMMARY OF RESULTS FOR COLD INJECTION

$\left|\frac{J_e}{J_i}\right|$

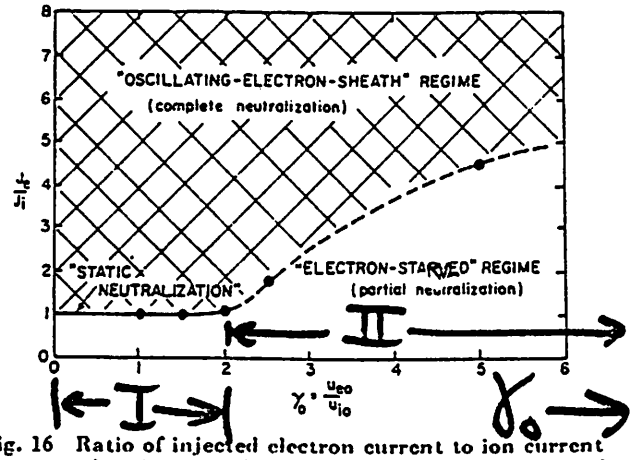

Fig. 16 Ratio of injected electron current to ion current for neutralization as a function of γ_0. Three regimes of operation are shown. The "static neutralization" regime is confined to the solid line up to $\gamma_0 = 2$. In the "electron-starved" regime ions return as in Fig. 13. In the "oscillating-electron-sheath" regime neutralization is obtained by the mechanism of Fig. 15.

Regimes
I. Static
II. Oscillating electron sheath.

MODELS OF PARTICLES AND MOVING MEDIA

DONALD A. DUNN

DEPARTMENT OF ENGINEERING-ECONOMIC SYSTEMS AND
INSTITUTE FOR PLASMA RESEARCH
STANFORD UNIVERSITY
STANFORD, CALIFORNIA

1971

ACADEMIC PRESS New York and London

Warm electron injection.

NOVEMBER 1963 AIAA JOURNAL VOL. 1, NO. 11

Computer Simulation of the Electron Mixing Mechanism in Ion Propulsion

O. BUNEMAN*
Stanford University, Stanford, Calif.
AND
G. KOOYERS†
Litton Industries, San Carlos, Calif.

A one-dimensional simulation with electrons and ions treated as sheet charges in mutual coulomb interaction and simplified emission conditions (ions are injected with uniform velocity through a plane accelerator grid, electrons with a thermal distribution from a plane decelerator grid at ship potential) was programmed into a digital computer. The dynamic buildup of the plasma is observed; the thrust seems to be maintained almost steadily, and good spontaneous neutralization seems to take place. Nonstatic space charge fields oscillating at the electron plasma frequency seem to provide the entropy increase needed for proper mixing.

L/l = the ratio of distance between the ion emitter and the accelerator grid to the distance between the accelerator grid and decelerator-emitter grid
$= 1/3$

M/m = ratio of ion mass to electron mass $= 1800$

φ_1/φ_0 = the ratio of the potential between the accelerator grid and the decelerator-emitter grid to the potential between the ion emitter and the accelerator grid
$= 0.4$

$kT/e\varphi_0$ = ratio of mean electron energy to potential difference between ion emitter and accelerator grid
$= 1/180$

η_i = number of ion sheets injected per time step

η_e/η_i = ratio of electron sheets injected per time step to the number of ion sheets injected per time step
$= 2$

N = the approximate number of ion sheets between the accelerator grid and the decelerator-emitter grid
$(N_D \cong 30, 60, 120, 240)$

The output variables from the computer are as follows:

φ_{ship}/φ_0 = the ratio of the integrated spaceship potential at each time step to φ_0

T_{actual}/T_{ideal} = the ratio of the force exerted on the ship by all the charged sheets to the ideal force on the ship calculated at each time step from the change in momentum one would expect if the ions left the ship with energy $\varphi_0 - \varphi_1$

φ_p/φ_0 = the ratio of φ_p the potential in the plasma to φ_0 as a function of distance from the accelerator grid; the potential is found by integrating the electric field in the plasma from the farthest out sheet to the accelerator grid

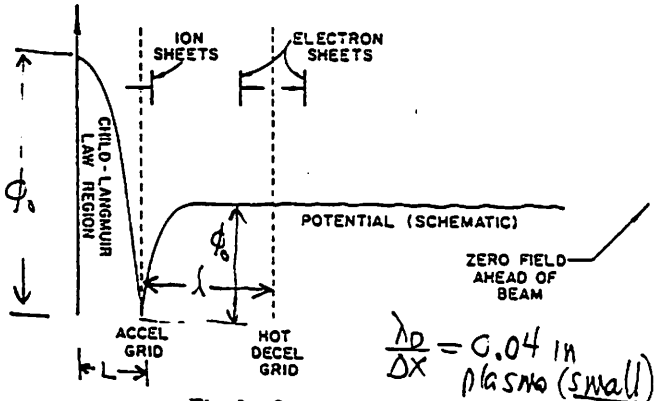

Fig. 1 One-dimensional model.

No collisions (hot decel grid intercepts 1/4 of electrons passing through)

{ 1 ion sheet injected, cold.
{ 2 electron sheets injected, warm

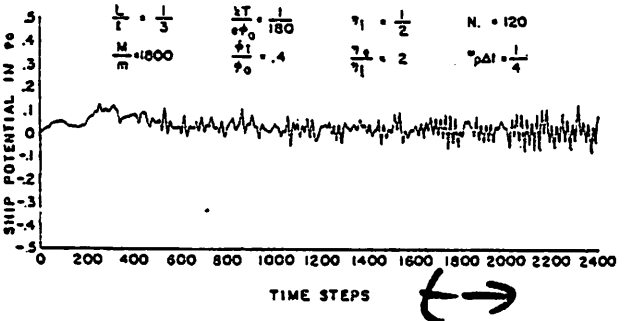

Fig. 2 Ship potential vs time, $N = 120$.

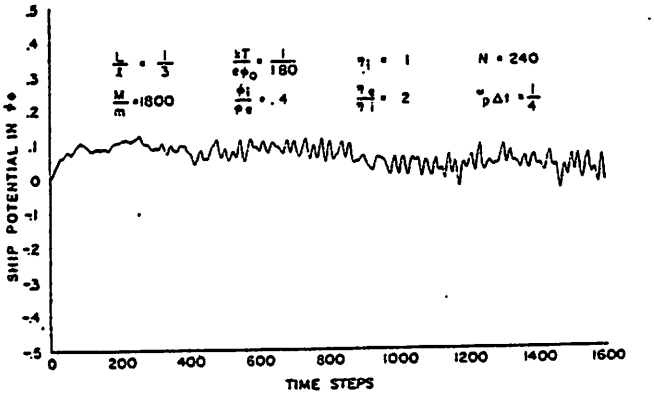

Fig. 3 Ship potential vs time, $N = 240$.

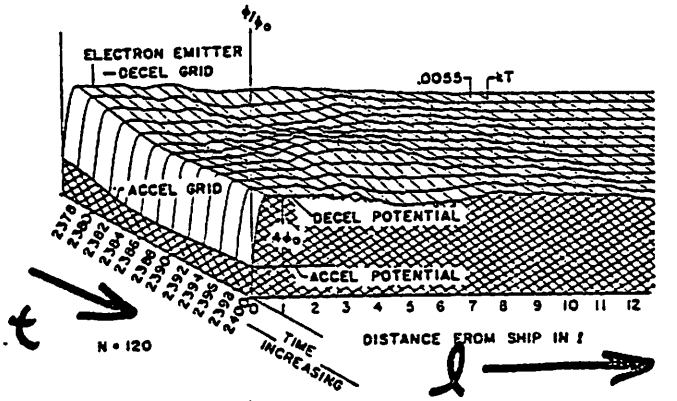

Fig. 4 Integrated potentials, time-distance plots, $N = 120$.

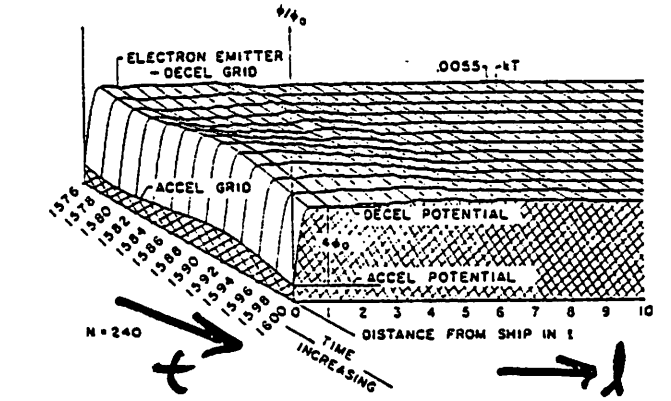

Fig. 5 Integrated potentials, time-distance plots, $N = 240$.

Large ϕ fluctuations, at ω_{pe}.

$|e\phi| \sim \frac{\text{ion energy}}{5}$

These provide good mixing of e and i.

Results

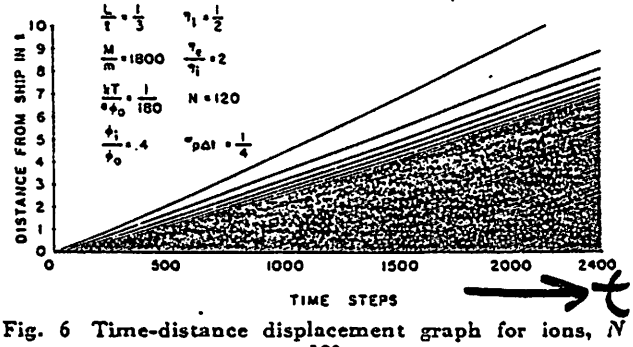

Fig. 6 Time-distance displacement graph for ions, $N = 120$.

NO ions returned

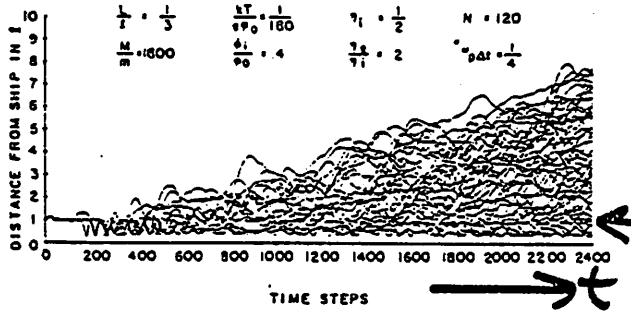

Fig. 7 Time-distance displacement graph for electrons, $N = 120$.

maybe a hot sheath at hot (electron) grid

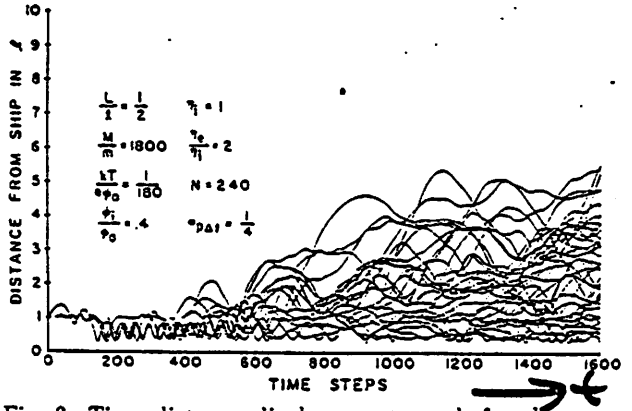

Fig. 8 Time-distance displacement graph for electrons, $N = 240$.

Two dimensional, warm e, cold i.

Two-Dimensional Computer Experiments on Ion-Beam Neutralization

R. P. WADHWA,* O. BUNEMAN,† AND D. F. BRAUCH‡
Litton Industries, San Carlos, Calif.

The two-dimensional electron-ion mixing mechanism for ion propulsion has been programed into a computer. Electrons and ions are simulated by several thousand rods of negative and positive charge. They are accelerated step-by-step, the space-charge fields being evaluated at each step by a new superfast technique of integrating Poisson's equation. The technique employs Fourier analysis, a marching method, and a capacitance matrix characterizing the electrode system. Integration takes approximately one second for 2% linear resolution. A stack of strip ion beams is injected through an accel-grid. Thermal electrons are released from both sides into each beam. The electron emitters define the decel-potential but are not placed directly within the beams; free space conditions are imposed at the heads of the advancing beams. Trajectory and equipotential plots show that the electron supply and demand of the beams is regulated by fluctuating fields. A near-neutral plasma is formed at a potential within a few kT of the electron emitters. The thrust is thus maintained near a value corresponding in ion acceleration to this potential, beam spread remaining negligible. Changing parameters, such as masses, currents, and velocities produce expected results, such as ion turn around when electron emission is reduced to zero value.

2d model

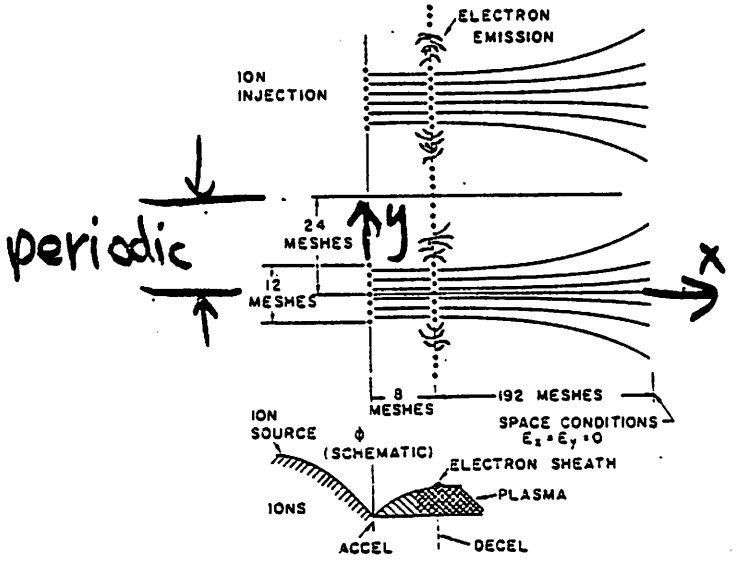

Fig. 1 A schematic of electron and ion injection in an ion engine.

Results

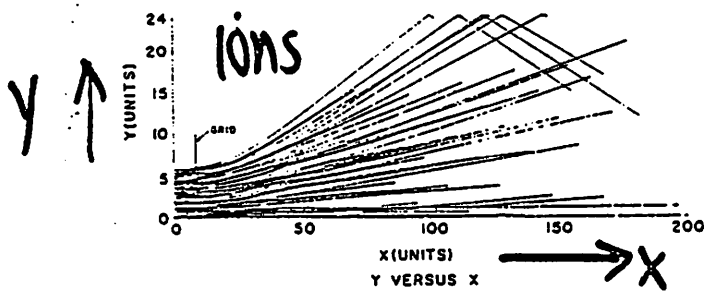

Fig. 2 Ion trajectories, Y vs X; $M/m = 144$, $l/L = 1.5$, $N_i = 3$, $N = 90$, $a/l = 0.75$, $\varphi_1/\varphi_0 = 0.4$, $N_e/N_i = 3$, $\omega_p\Delta t = 0.28222$, and $e\varphi_0/kT = 14.4$.

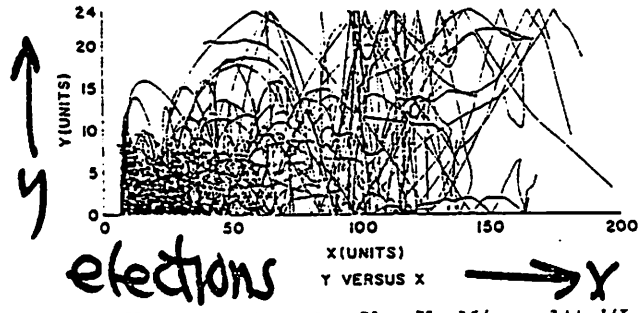

Fig. 3 Electron trajectories, Y vs X; $M/m = 144$, $l/L = 1.5$, $N_i = 3$, $N = 90$, $a/l = 0.75$, $\varphi_1/\varphi_0 = 0.4$, $N_e/N_i = 3$, $\omega_p\Delta t = 0.28222$, and $e\varphi_0/kT = 14.4$.

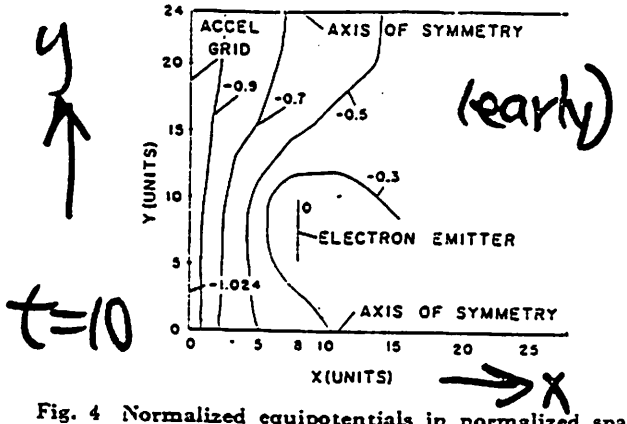

Fig. 4 Normalized equipotentials in normalized space; time step: 10 $M/m = 144$, $l/L = 1.5$, $N_i = 3$, $N = 90$, $a/l = 0.75$, $\varphi_1/\varphi_0 = 0.4$, $N_e/N_i = 3$, $\omega_p\Delta t = 0.28222$, and $e\varphi_0/kT = 14.4$.

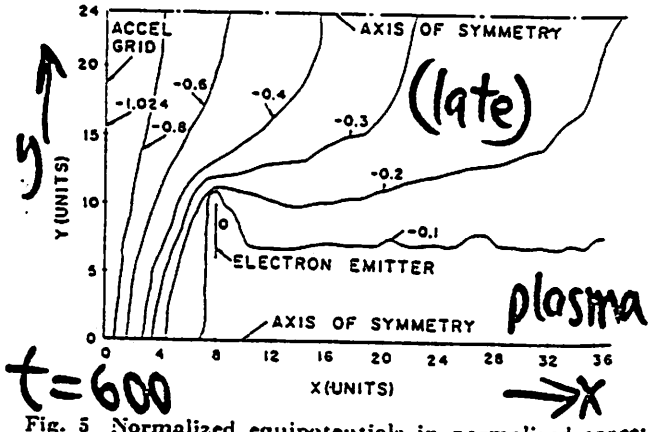

Fig. 5 Normalized equipotentials in normalized space; time step: 600; $M/m = 144$, $l/L = 1.5$, $N_i = 3$, $N = 90$, $a/l = 0.75$, $\varphi_1/\varphi_0 = 0.4$, $N_e/N_i = 3$, $\omega_p\Delta t = 0.28222$, and $e\varphi_0/kT = 14.4$.

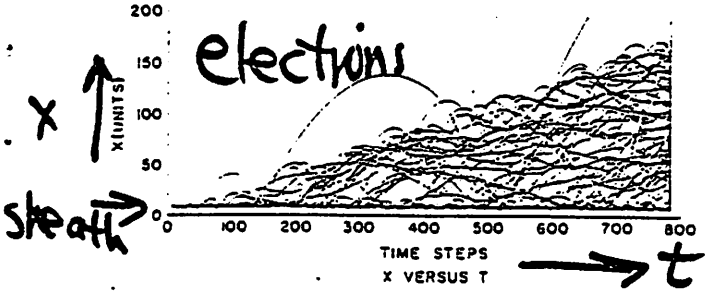

Fig. 6 Electron trajectories. X vs T; $M/m = 256$, $l/L = 1.125$, $N_i = 3$, $N = 90$, $a/l = 0.75$, $\varphi_1/\varphi_0 = 0.4$, $N_e/N_i = 4$, $\omega_p\Delta t = 0.2822$, and $e\varphi_0/kT = 25.6$.

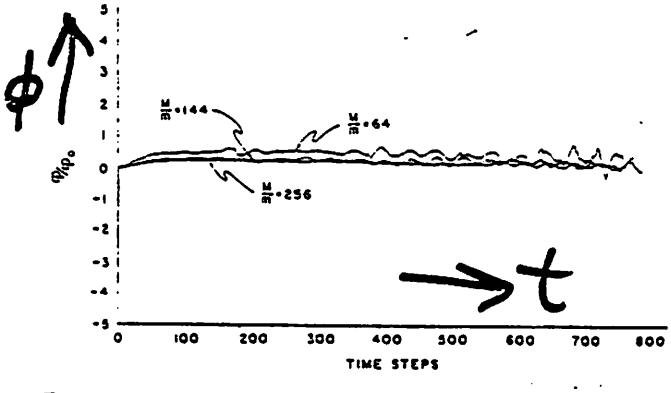

Fig. 8 Ship potential vs time; variation with mass; $N_i = 3$, $N = 90$, $a/l = 0.75$, $\varphi_1/\varphi_0 = 0.4$, $N_e/N_i = 4$, and $\omega_p\Delta t = 0.2822$.

Like Dunn & Ho "plasma bottle". Sheath, virtual cathode fluctuations regulate supply of electrons

Oscillations at ω_{pe}

EXPERIMENTAL OBSERVATION OF e and i OSCILLATION BURSTS.

High-Frequency Oscillations in a Thermal Plasma

WILLIAM H. CUTLER
Hansen Laboratories of Physics, Stanford University, Stanford, California
(Received 3 September 1963)

Journal Applied Physics 35 pp 464-465 (1964)

LOW-FREQUENCY ion oscillations are frequently observed in thermal plasma devices, such as power converter plasma diodes,[1] and are associated with drift of the plasma electrons. Birdsall and Bridges[2] have suggested that an instability of the drifting electrons should give rise to high-frequency oscillations with period near the electron transit time across the device, and that such oscillations decrease the average electron current and density. Relaxation of the resultant charge imbalance would produce a cycle of the ion oscillation.

Oscillations of this type have been observed in a thermal cesium plasma. The apparatus is a cesium-vapor diode utilizing a 1.27-cm-(½-in.) diam electron-bombardment-heated tungsten button, opposed by a moveable cold plate, operating in an axial magnetic field.

With the diode short circuited and the button temperature such that an excess of ions is available, smooth ion oscillations are observed as diode current fluctuations with frequency depending only on the button-to-plate spacing. In addition, an L-C circuit and detector picks up a signal with frequency 500 to 1000 times higher occurring in bursts once each cycle of the lower frequency fluctuation. Figure 1, prepared from oscilloscope photographs, shows the waveform of the low-frequency fluctuations and the envelope of the high-frequency bursts. (The small pips of alternating sign occurring in the detector output are the low-frequency current fluctuations, differentiated by the coupling coil).

Table I lists the observed low and high frequencies as a function of diode spacing.

The high-frequency bursts always occur in conjunction with the low-frequency fluctuations. The detailed shape of the high-frequency envelope may vary somewhat as conditions are changed, but the burst always occurs slightly before or at the onset of each low-frequency current puise. The higher frequency is 500 to 1000 times the lower, this ratio being near the square root of the ion-electron mass ratio.

TABLE I. Oscillation frequency and burst frequency as a function of diode spacing.

Diode spacing	Oscillation frequency	Burst frequency
0.56 cm	100 kc/sec	86 Mc/sec
0.73	76	65
0.89	61	50
0.96	52	48
1.25	45	43
1.35	39	35
1.54	37	34
1.89	30	31

f_{low} f_{high}

$$\frac{f_{high}}{f_{low}} = 500 + 1000$$

$$\left(\sqrt{\frac{M_{Cs}}{m_e}} = 492\right)$$

[1] K. P. Luke and F. E. Jamerson, J. Appl. Phys. 32, 321 (1962).
[2] C. K. Birdsall and W. B. Bridges, J. Appl. Phys. 32, 2611 (1961).

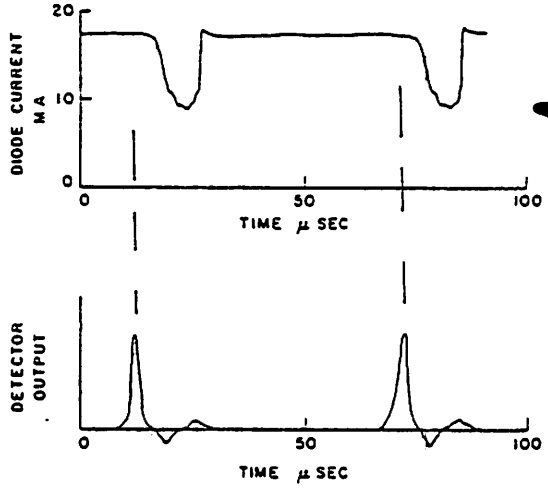

FIG. 1. Waveform of low-frequency fluctuations and the envelope of high-frequency bursts.

← waveform of low-frequency fluctuations

← envelope of high-frequency bursts, always precedes low frequency, always occur with low frequency fluctuation

DIODE SIMULATIONS ; NO STEADY STATE

Nonexistence of dc States in Low-Pressure Thermionic Converters

PETER BURGER*
Stanford University, Stanford, California
(Received 24 April 1964)

Journal Applied Phys.
35 pp3048-3049, 1964.

Warm e
Warm i

$$\alpha \equiv \left(\frac{J_{si}}{J_{se}}\right)\left(\frac{m_i}{m_e}\right)^{1/2}$$

(a)

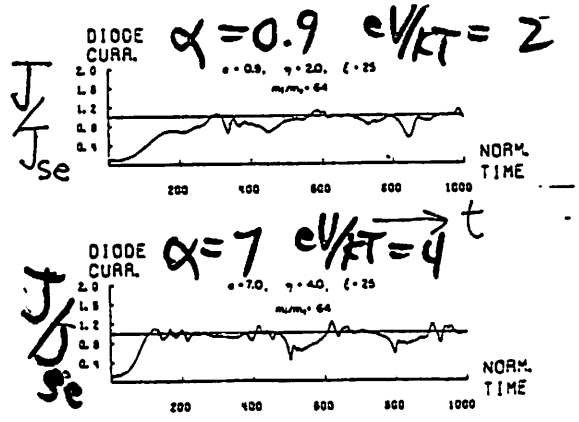

FIG. 1. The normalized diode current in the computer simulated converter for two cases that were included in McIntyre's dc analysis. The normalized current of value 1.0 is the expected direct current for both cases.

$\frac{d}{\lambda_D} = 25$, $\frac{m_i}{m_e} = 64$

(b)

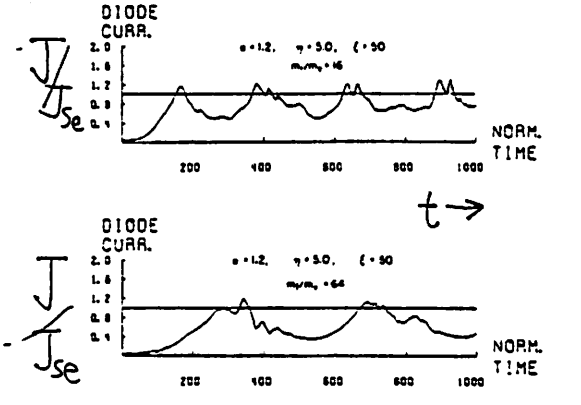

FIG. 2. Fluctuations of the current in the computer simulated diode that approximates an experimental cesium diode (Ref. 8). Comparison of the two curves shows the effect of the mass ratio m_i/m_e on the fluctuations. A normalized current of value 1.0 is again the expected direct current in the diode.

$\frac{m_i}{m_e} = 16$

$\frac{m_i}{m_e} = 64$

} Like experimental diode of Cutler; see two frequencies, high connected with electron transit time; low, with ion time.

$\alpha = 1.2$, $\frac{eV}{KT} = 5$, $\frac{d}{\lambda_D} = 50$

Conclusion: for large electron currents, no dc (time indep.) state

Some speculation:

JOURNAL OF APPLIED PHYSICS VOLUME 35, NUMBER 11 NOVEMBER 1964

Regular Articles

Nature of Spontaneous Oscillations in a Cesium Diode Energy Converter*

W. T. Norris†
Research Laboratory of Electronics, Massachusetts Institute of Technology, Cambridge, Massachusetts
(Received 12 May 1964)

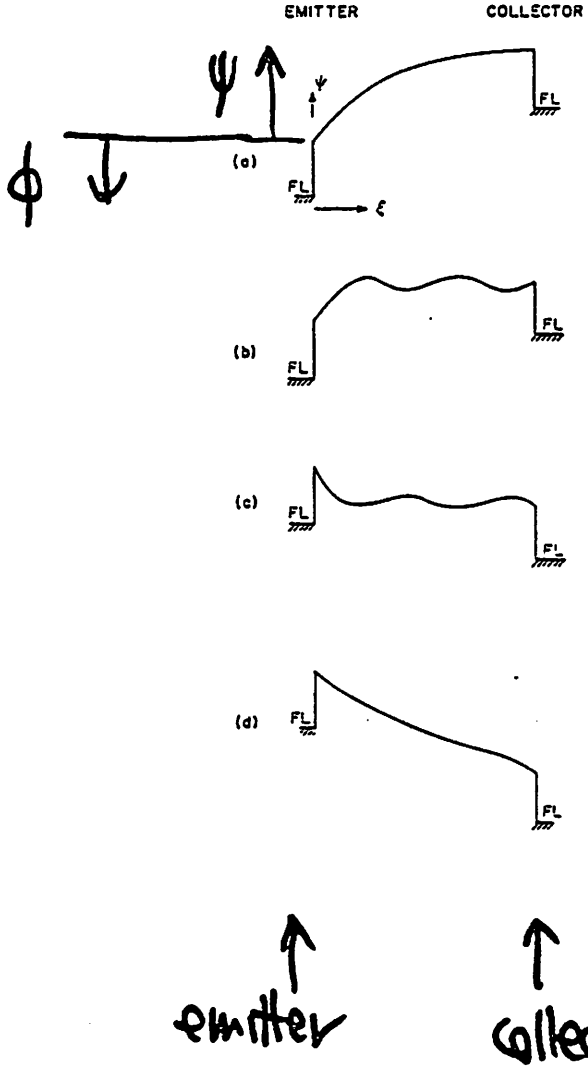

FIG. 10. Steady-state distribution curves: (a) Shows no electron instability, (b) and (c) probably will show electron instability, and (d) is probably electron stable.

$\psi = q\phi$

Signed

emitter

collector

WARM e, WARM i ; "2 dc states", oscillatory.

JOURNAL OF APPLIED PHYSICS VOLUME 36, NUMBER 6 JUNE 1965

Theory of Large-Amplitude Oscillations in the One-Dimensional Low-Pressure Cesium Thermionic Converter

PETER BURGER
Institute for Plasma Research, Stanford University, California
(Received 20 August 1964; in final form 18 March 1965)

The large-amplitude oscillations in a one-dimensional, low-pressure cesium thermionic converter are analyzed. With the help of results obtained from computer calculations designed to simulate the operation of the converter, the current oscillations are explained in terms of the changing forms of the potential distribution in the system. The variations in the form of the potential function are explained by means of the concept of a "temporary dc state." Such a state differs from the ideal self-consistent state in that the electrons and the potential adopt new distributions while the ion distribution stays the same as in the self-consistent state. In fact, the ions are treated as too heavy to respond to the new potentials while the electrons adjust themselves rapidly to them. The existence of a temporary dc state is decided by solving a static problem only; but if such a state exists, then there is a possibility for relaxation-type oscillations in the system with frequencies characteristic of the ions.

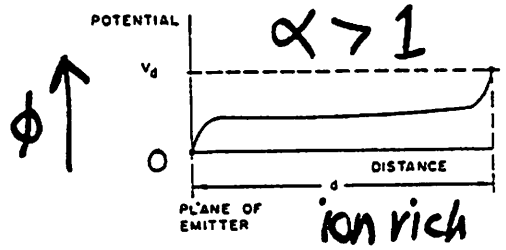

FIG. 2. Expected dc potential distribution in the converter for slightly ion-rich operation $[J_{si}/J_{se} > (m_e/m_i)^{\frac{1}{2}}]$ and a positive applied potential on the collector.

at V_d

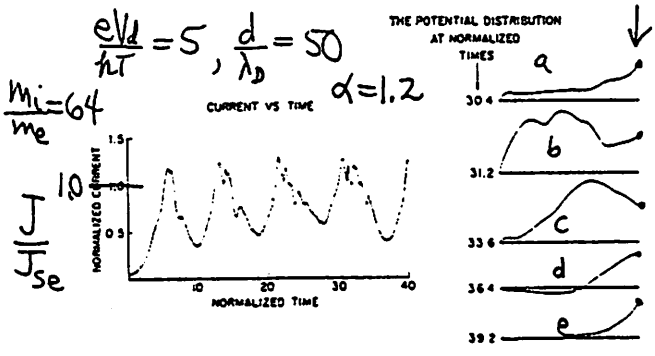

FIG. 3. Characteristics of the computer-simulated converter. Time is normalized to the average transit time of the electrons, current is normalized to their saturation current.

30.4 (a) to 31.2 (b) = 0.8 d/v_{te}

at b, ions returned to emitter so φ drops as in c, d and pot. min forms, so J_e lower. Ions fill min. and cycle begins again.

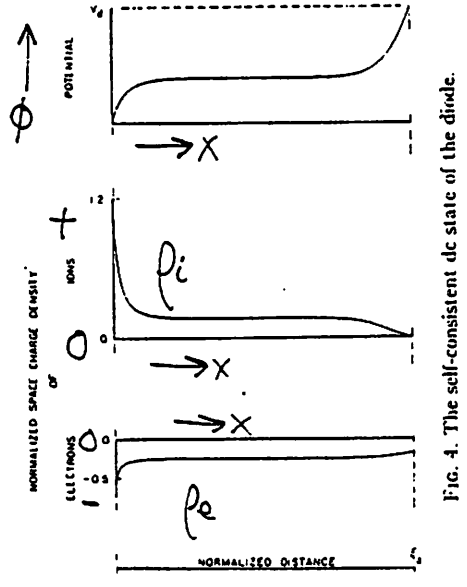

FIG. 4. The self-consistent dc state of the diode.

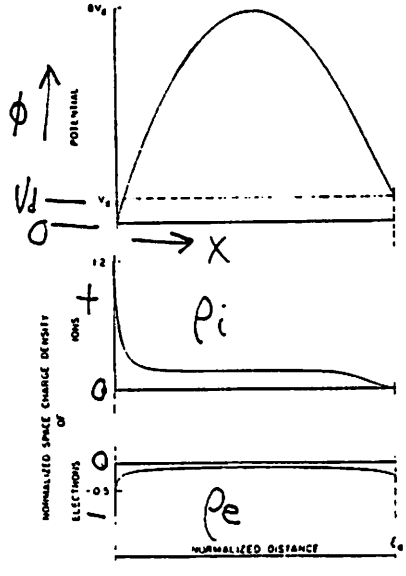

FIG. 5. The temporary dc state of the diode. The space-charge-density function of ions is the same as that in Fig. 4, but the space-charge-density function of electrons is rearranged so that the electron space charge is self-consistent with the new form of the potential function.

Self consistent dc state
$\frac{d}{\lambda_D} = 50$, $\frac{eV_d}{KT} = 5$, α = 1.2

"temporary" dc state, same $\rho_i(x)$ (frozen)
Accounts for large amplitude, low frequency oscillations seen in laboratory

DIODE; e and i created within diode, uniformly. no beam

THE PHYSICS OF FLUIDS VOLUME 8, NUMBER 12 DECEMBER 1965

Computer Experiments on the Randomization of Electrons in a Collisionless Plasma

P. BURGER, D. A. DUNN, AND A. S. HALSTED*
Institute for Plasma Research, Stanford University, Stanford, California
(Received 23 June 1965)

The large-signal, time-dependent behavior of a one-dimensional, collisionless plasma is simulated on a computer by calculating the trajectories of a large number of charge sheets in a one-dimensional space. The equations of motion of the charge sheets are calculated self-consistently with the electric fields that the charges themselves set up in the diode. A plasma is formed in the diode by the generation of electron and ion sheets at a constant rate in time and space. The velocity distribution, charge distribution, and potential distribution of the simulated plasma are investigated. Electrons and ions are generated with prescribed initial velocities. Because of the heavy mass of the ions, the potential in the middle of the diode becomes positive with respect to the wall. The potential does not settle down to a dc state, however, but exhibits fluctuations at the electron plasma frequency. It is shown that these rf fluctuations randomize the velocities of the electrons. A clear similarity is shown between the effects of these rf fluctuations and elastic collisions.

dc sheath

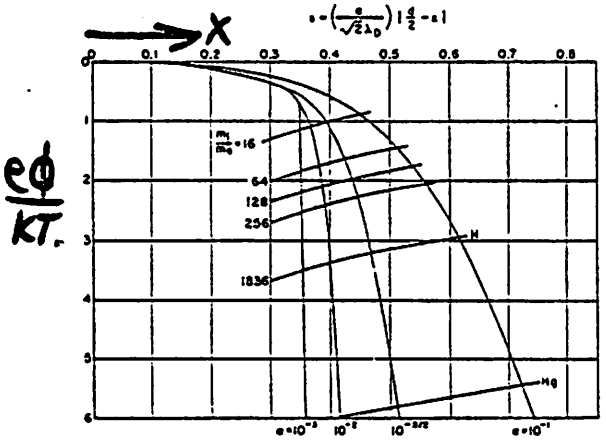

$\frac{e\phi}{KT_e}$

FIG. 2. Potential versus distance curves of static theory as calculated by Dunn and Self.[12]

[12] D. A. Dunn and S. A. Self, J. Appl. Phys. 35, 113 (1964).

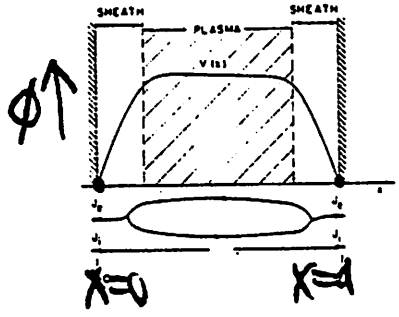

dc state

FIG. 1. Expected dc state of a one-dimensional plasma generated between two metal walls at the same potential.

expected.

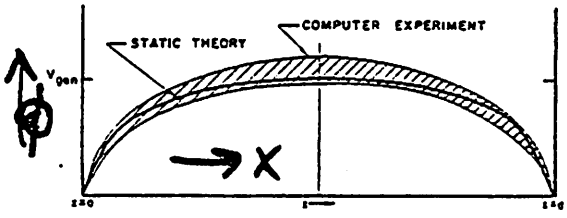

FIG. 4. The region of the fluctuating potential versus distance functions in the computer-simulated diode. The solic line shows the potential function calculated by static theory.

(note: small m_i/m_e reduces sheath drop in ϕ)

all e created at same speed, both directions, v_{gen}

$\alpha \approx \frac{\lambda_D}{d}$

Ions created at rest.

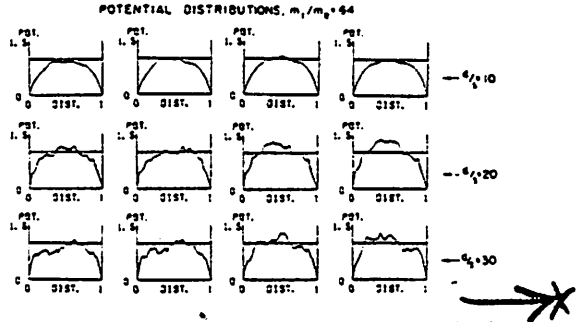

ϕ

FIG. 5. The potential versus distance functions in the computer-simulated diode for three different diodes.

ϕ peak oscillates back and forth across diode, at ω_{pe}

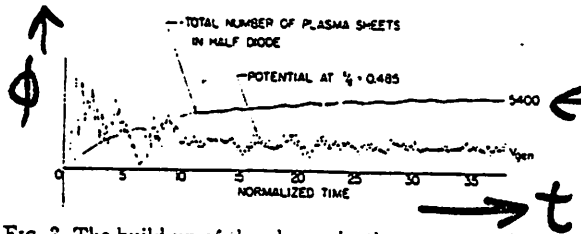

FIG. 3. The build up of the plasma in the computer-simulated diode. Time is measured in units of t_{gen}.

sheets in half diode

ϕ fluctuates at ω_{pe}

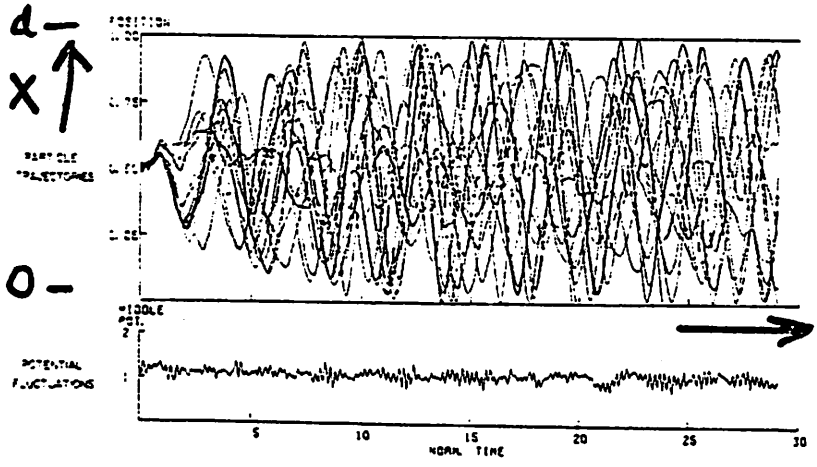

particles that start at $x = d/2$ at rest.

FIG. 7. The randomizing effect of the potential fluctuations on test particles that start from rest at the middle of the plasma. The parameters for this case were $m_i/m_e = 64$, $d/s = 20$.

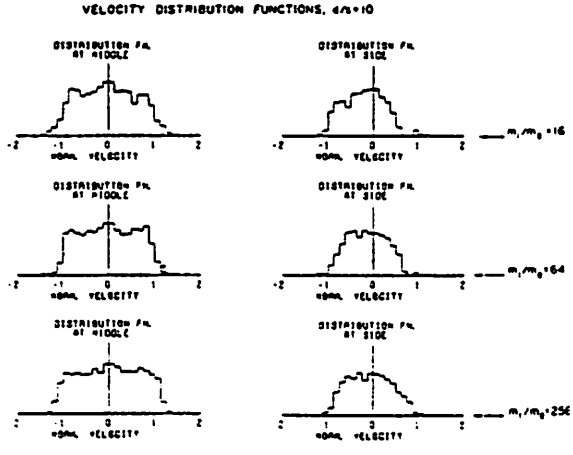

FIG. 12. The velocity distribution functions of the electrons at the middle of the diode and at the left wall for three different diodes.

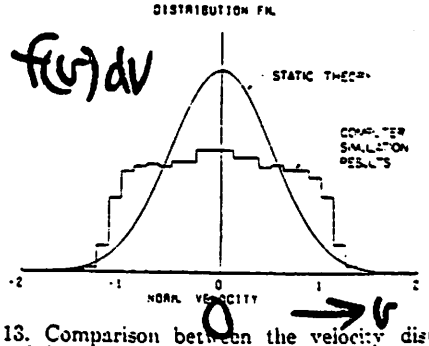

FIG. 13. Comparison between the velocity distribution functions of the electrons of static theory and of the computer experiments at the middle of the plasma.

$f(v)\,dv$ at $x = \frac{d}{2}$

$f(v)\,dv$ at left wall, depleted on right due to removal of e striking right wall

Simulation shows:

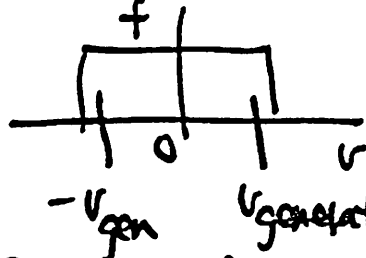

Conclude: rf randomization different from usual collisions

EXPERIMENTS ; OSCILLATIONS

JOURNAL OF APPLIED PHYSICS VOLUME 37, NUMBER 7 JUNE 1966

Oscillations in the Thermal Cesium Plasma Diode*

WILLIAM H. CUTLER† AND PETER BURGER
Institute for Plasma Research, Stanford University, Stanford, California
(Received 10 September 1965; in final form 23 February 1966)

Oscillations with frequencies corresponding to ion transit times are observed in thermal cesium diodes having parallel-plane construction. Electrons and ions are emitted from heated flat tungsten disks immersed in cesium vapor. Measurements are made with one emitter facing a cold collector and also with two emitters facing each other. Large-amplitude oscillations are observed whenever the collector potential is large enough to draw electron saturation current through the diode. Characteristics of these oscillations are well correlated with computer-simulated results and explained by theory developed earlier. High-frequency bursts during some parts of the low-frequency fluctuations are also observed as predicted from current-vs-time curves of the computer-simulated diode. The electron-rich and ion-rich regimes of the two-emitter diode are found and switching between the two regimes is demonstrated by measuring the ion saturation current with a probe at the middle of the diode.

Find that (a la Norris, 1964 and Burger, 1961) oscillations "are due to rapid rearrangement of potential distribution in the diode, made possible by electron motion due a time interval when ions remain comparatively at rest."

Rule out: (a) ion acoustic wave instability
(b) multiple dc states plus jumps between states

Devices:

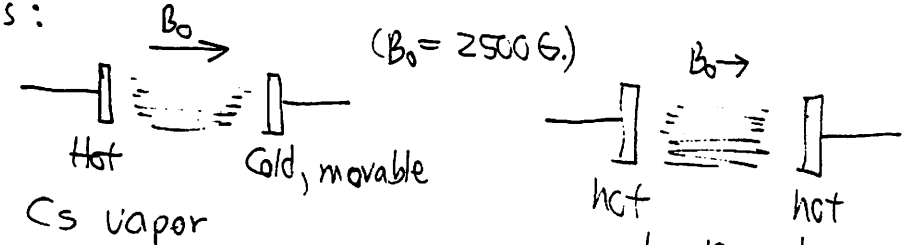

$$\alpha \equiv \frac{J_{si}}{J_{se}} \left| \frac{m_i}{m_e} \right|$$

$\alpha > 1$ is "ion rich" at emitter

ION RICH

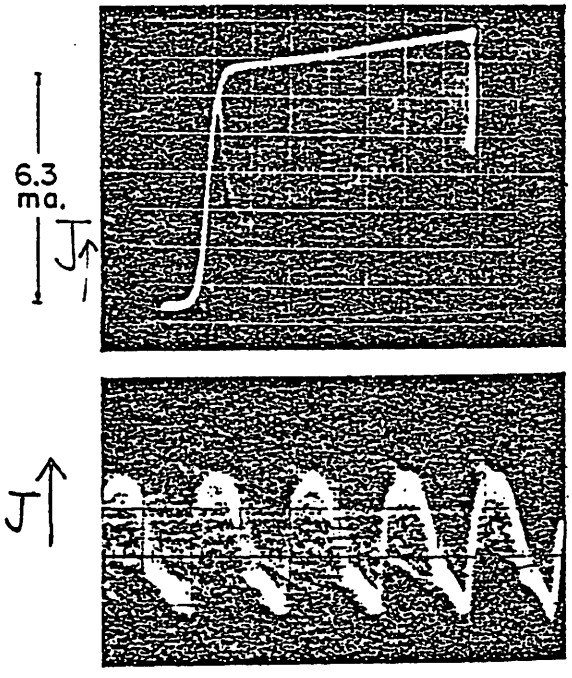

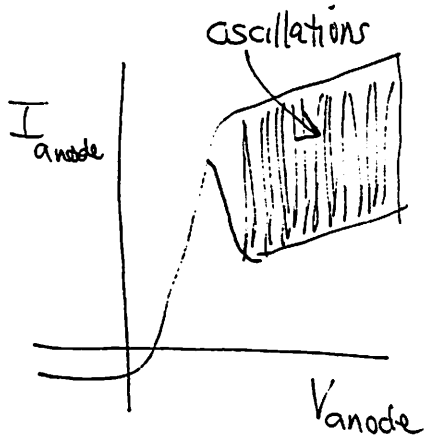

FIG. 3. Anode current vs anode voltage (upper trace), and anode current vs time (lower trace) for strongly ion-rich operation.

ELECTRON RICH

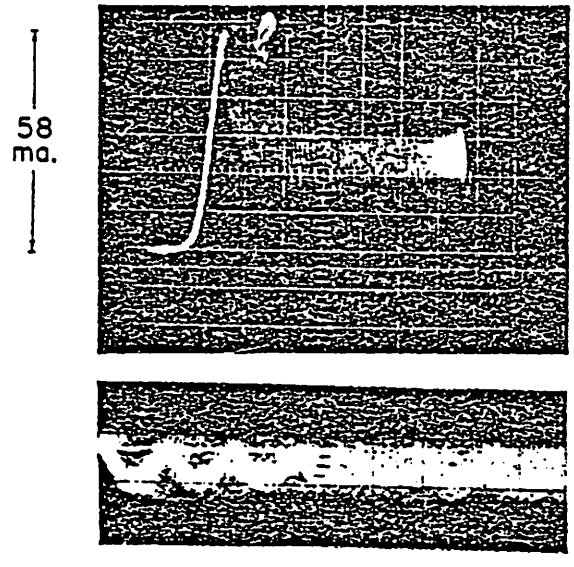

FIG. 4. Anode current vs anode voltage and time for large electron emission.

Single ended

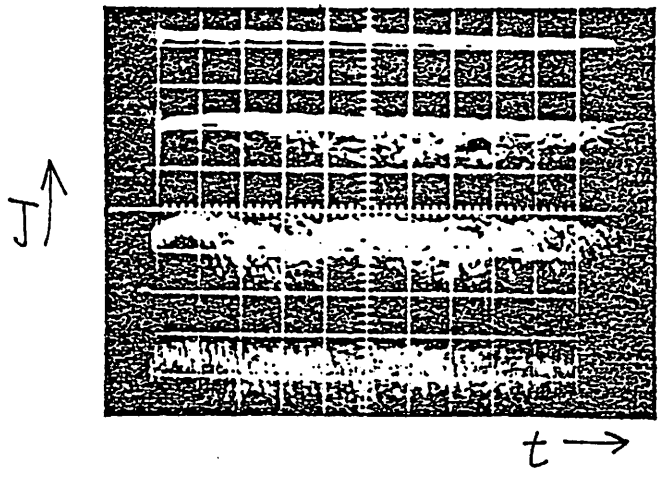

(a) large electron emission $\alpha \lesssim 1$

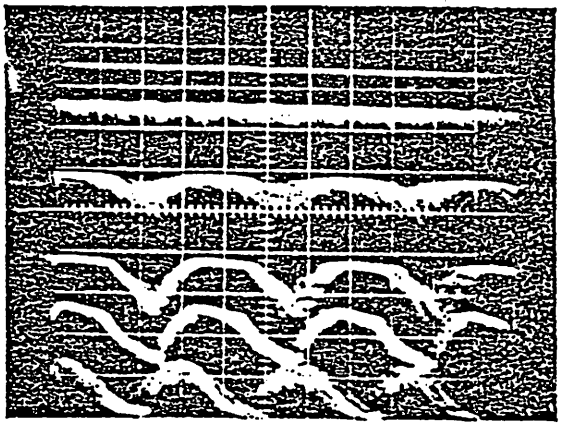

(b) Most Common oscillation $\alpha \approx 1$

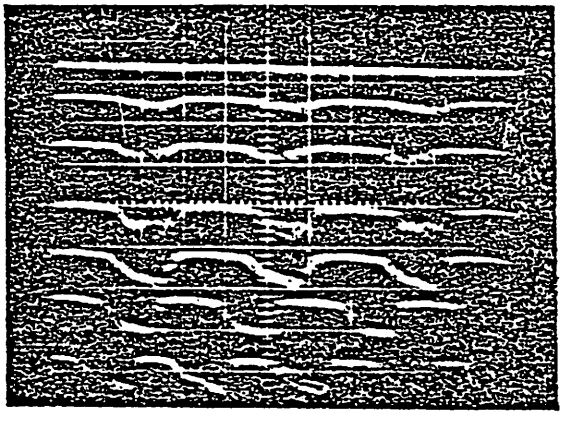

(c) ion rich $\alpha > 1$

FIG. 5. Oscilloscope traces of diode current vs time for increasing anode potentials. (a) Large electron emission (α might be slightly less than unity). (b) The parameter α is of the order of unity. (c) Heavily ion-rich condition.

Single ended

Experiment

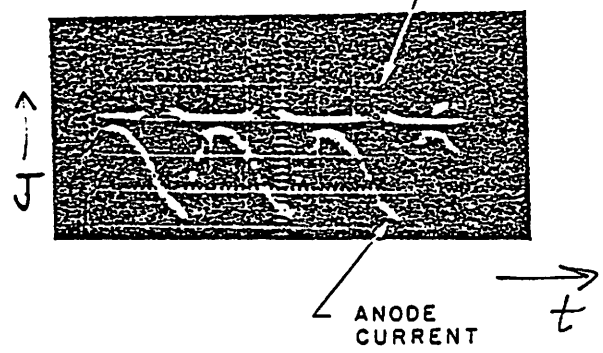

FIG. 6. Observed high-frequency bursts along with the low-frequency oscillations of the diode current.

ω_{high} is 500 to 1000 ω_{low} for Cs, $T_{Cs} = 492 T_e$ transit times

Bursts "occur just before and during the initial drop in the diode current",

"indicating bursts are a manifestation of electron transit phenomena." "Bursts are always present when the low-frequency oscillation occurs, and never occur alone."

Bursts are at a few MHz, due to the large spacing.

Simulation

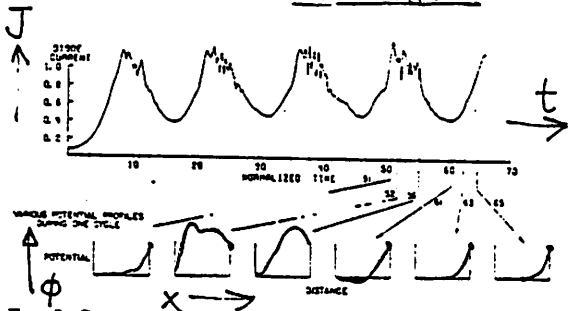

FIG. 7. Current vs time in the computer-simulated diode. The potential distributions in the diode are also shown at different times during one cycle of oscillations. The mass ratio $m_i/m_e = 256$ for these calculations.

$\frac{m_i}{m_e} = 256$, $\frac{T_i}{T_e} = 16$

$\omega_{high} \simeq 26\, \omega_{main}$

$d = 5\pi\lambda_D$

More details given to back up model postulated.

Single ended.

Found excellent agreement between experiment and simulation.

Zero-Field Solutions and Their Stability in the One-Dimensional Low-Pressure Cesium Diode

PETER BURGER
Institute for Plasma Research, Stanford University, Stanford, California
(Received 31 May 1966; in final form 9 March 1967)

(Simulation)

The dc potential solutions which have zero slope at the emitter are calculated and examined for the low-pressure cesium diode. It is assumed that ions and electrons are emitted thermionically at the emitter with a given ratio of ion-to-electron saturation currents and a positive dc potential is applied to the collector. Furthermore, the potential is nowhere negative in the diode and electron saturation current flows through it. This assumption limits the range of α's to $0<\alpha<1$, where α is the ratio of ion-to-electron saturation currents times the square root of the ratio of their masses. It was found by Auer and Hurwitz that monotonically increasing potential solutions can exist only for the range of α's, $0<\alpha<0.405$. In the range $0.35<\alpha<0.405$ we found large amplitude oscillations in the diode by computer simulation methods. The static solutions for $\alpha<0.35$ were found stable. For $1>\alpha>0.405$ the static potential solutions have a long zero slope region within the diode or become periodic in space. All these solutions were found unstable and nonexistent in the diode that operates under time-varying conditions just as predicted by Auer and Hurwitz.

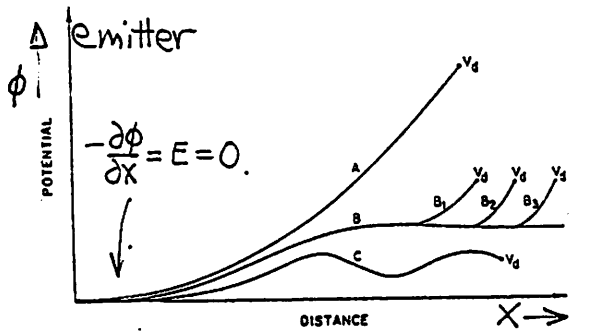

FIG. 1. The possible types (A, B, and C) of static zero-field solutions in the low-pressure cesium diode which allow electron saturation current to flow through the diode.

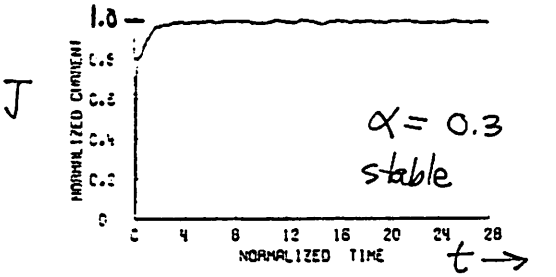

FIG. 6. Normalized current J/J_{se} vs normalized time $t(kT/m)^{1/2}/d$ in the computer-simulated diode for the zero-field parameters $d/\lambda_{DB}=30$, $eV_d/kT=42.6$, $\alpha=0.3$. The time step for calculations was 1/30 normalzed time unit and there are an average of 4000 sheets in the diode. Ion-to-electron mass ratio $M/m=64$.

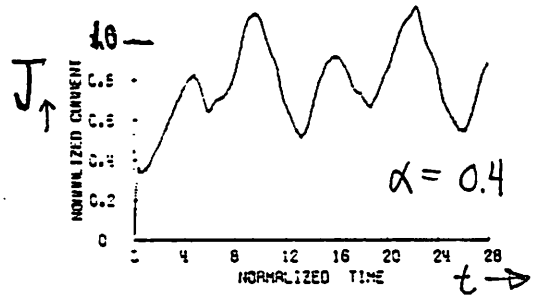

FIG. 7. Normalized current vs normalized time in the computer-simulated diode for the zero-field parameters $d/\lambda_{DB}=30$, $eV_d/kT=20.3$, $\alpha=0.4$. The average ion transit time is eight normalized time units.

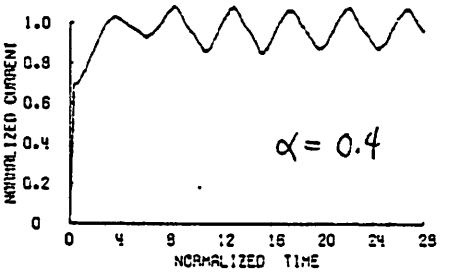

FIG. 8. The effect of increasing collector potential on the current-vs-time characteristics of the simulated diode (cf. Fig. 7). Same diode parameters as in Fig. 7 except $eV_d/kT=40$.

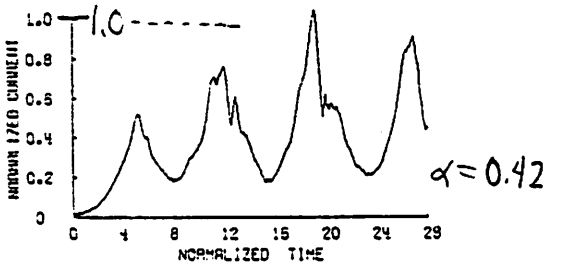

FIG. 9. Normalized current vs normalized time characteristics in the computer-simulated diode with parameters $d/\lambda_{DB}=100$, $eV_d/kT=5$, $\alpha=0.42$. An attempt to find the type-B zero-field solution in the diode with $eV_d/kT=1.8$ failed, and even with this higher collector potential, electron saturation current does not flow in the diode. TYPE B NOT FOUND

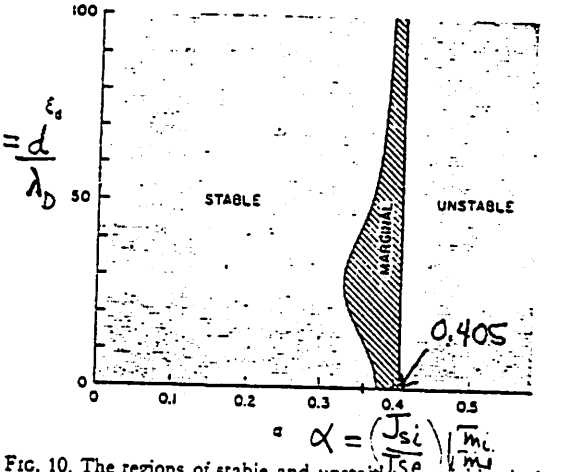

Agrees with Auer and Hurwitz (1959)

FIG. 10. The regions of stable and unstable zero-field solutions in the low-pressure cesium diode. For $\alpha>0.405$, type-A solutions are not possible, and the diode does not have a stable zero-field solution. In the range $0.35<\alpha<0.4$, large-amplitude oscillations start in the diode when the type-A zero-field solutions are set up.

FLUID SOLUTION; SHEATH

J. Plasma Physics (1981), *vol.* 25, *part* 3, *pp.* 373–389 June
Printed in Great Britain

On the temporal development of a plasma sheath

By J. W. CIPOLLA, Jr.† AND M. B. SILEVITCH‡
Northeastern University, Boston, Massachusetts 02115

(Received 22 May 1980 and in revised form 10 September 1980)

In this work we study a one-dimensional model for the time-dependent behaviour caused by placing an uncharged conducting surface in contact with a uniform equilibrium plasma. Both the probe potential and plasma response are unknown *a priori* but are specified through a set of self-consistent model equations and boundary conditions. We investigate some numerical and analytical consequences of this model. In particular, we consider such issues as (i) the formation and expansion of a quasi-neutral region connecting the non-neutral sheath to the distant undisturbed plasma; (ii) the validity of assuming the existence of a sheath edge; and (iii) the role of both static and dynamic Bohm criteria in the theory of unsteady sheath development.

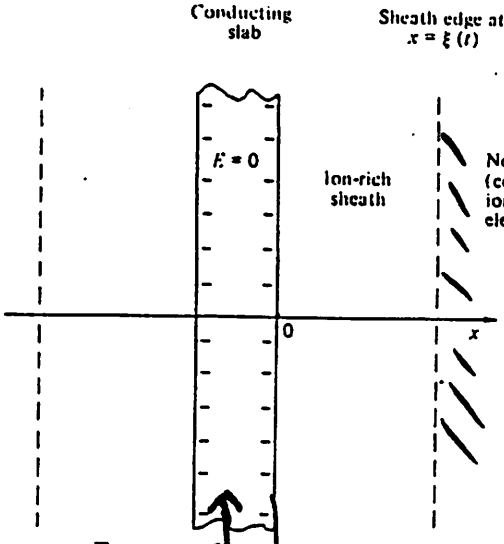

FIGURE 1. Geometry of the model.

cold i $T_e >> T_i$
Warme

x $x>0$ studied

metal slab, absorbs all incident charge
no emission

$N_e(\Phi) = N_0 \exp\{+|e|\Phi/kT_e\}$
$\Psi \equiv -|e|\Phi/kT_e$
} not correct at early times when electrons move quickly away from plasma

number flux $J_e(x=0,t) \equiv -N_0\left(\frac{kT_e}{2\pi m_e}\right)^{1/2} \exp[-\psi(x=0,t)]$ (used at $x=0$ only)

$(\psi = -e\phi)$

$\psi \uparrow$

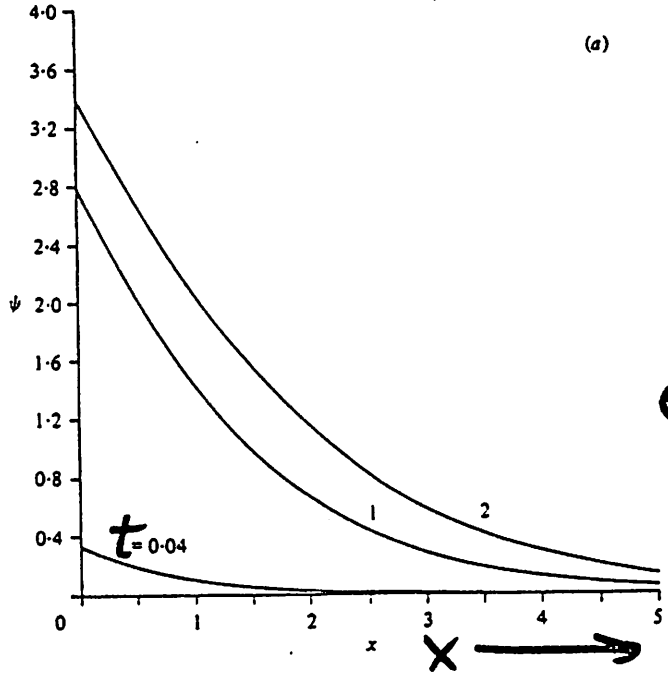

early

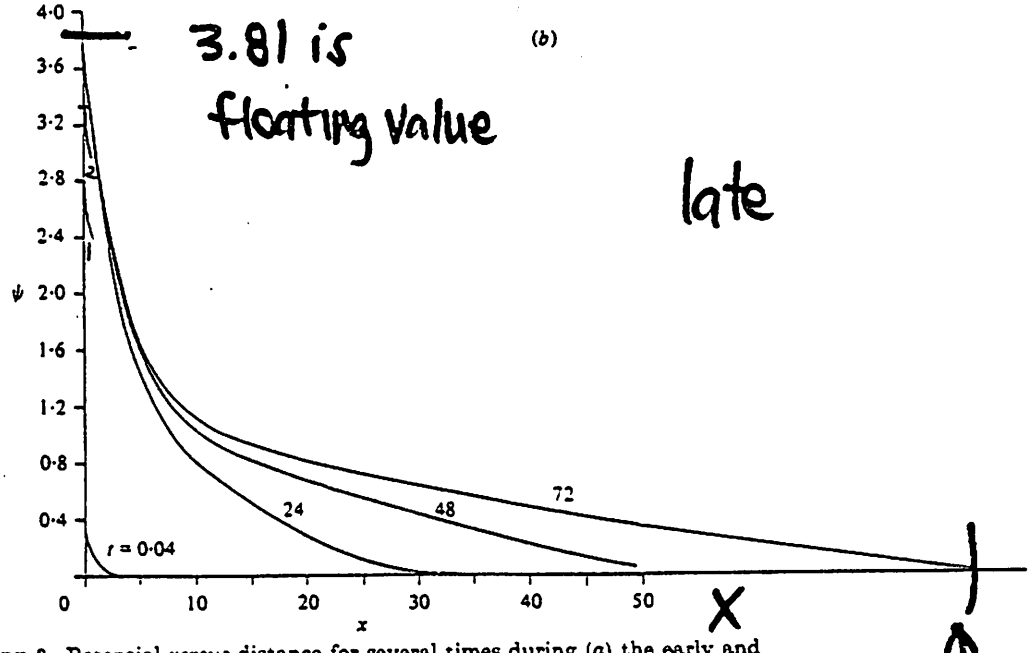

3.81 is floating value

late

$\uparrow \psi$

$\uparrow$

FIGURE 3. Potential *versus* distance for several times during (*a*) the early and (*b*) the later stages of development.

$\psi(80) = 0$

Extremely rapid fall of $\phi(t)$ at $x=0$

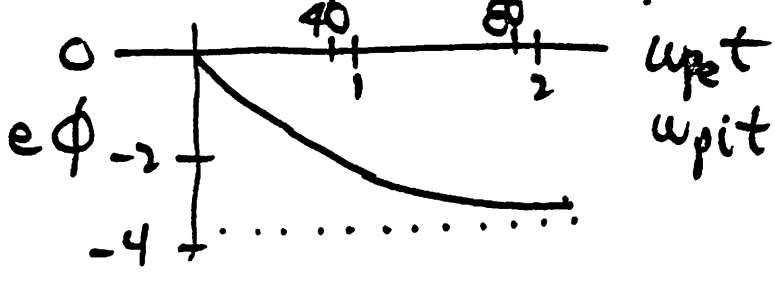

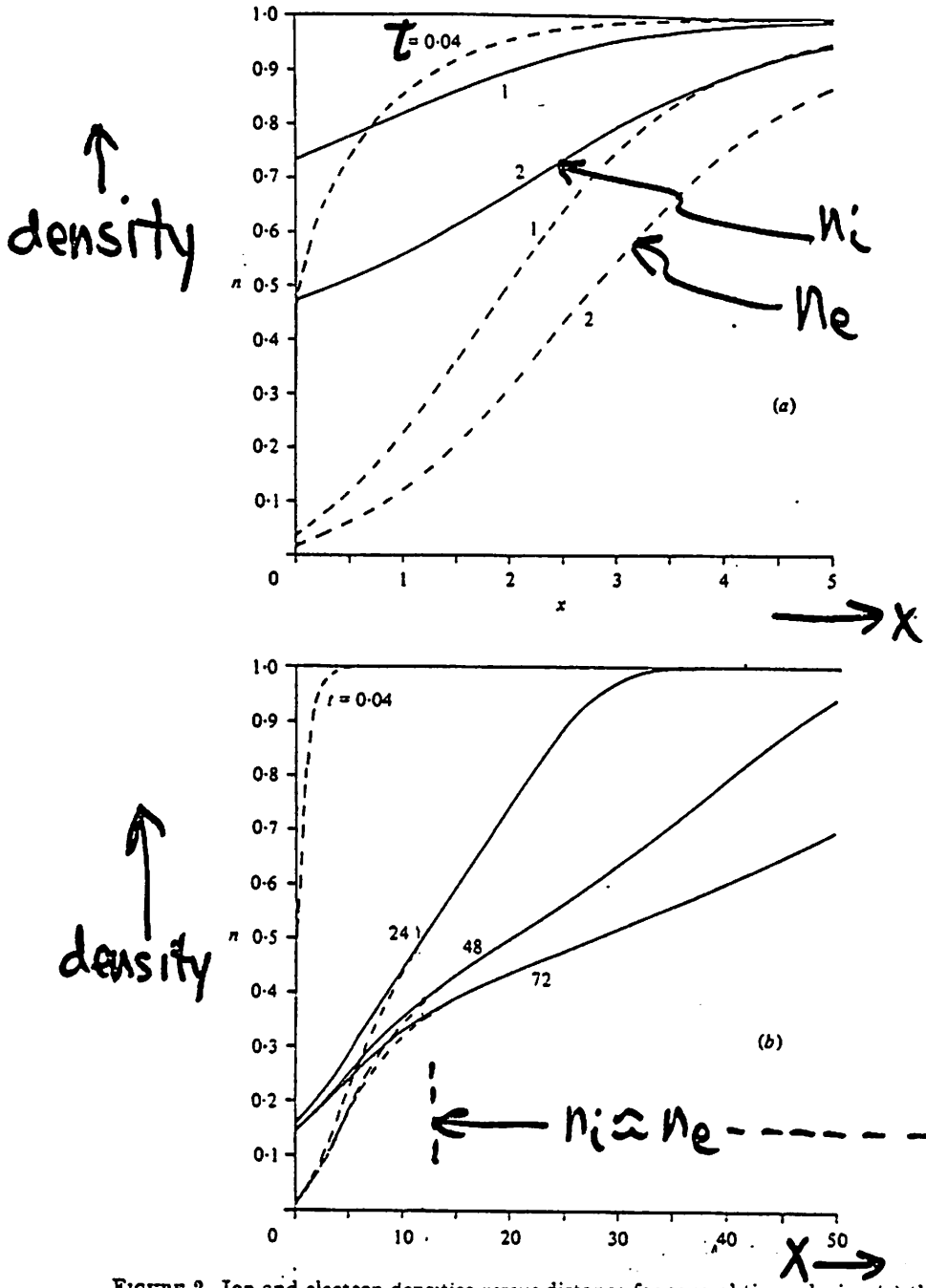

FIGURE 2. Ion and electron densities *versus* distance for several times during (*a*) the early and (*b*) the later stages of development. Electron densities are shown dotted.

t is $\frac{t}{\omega_{pi}}$

x is $\frac{x}{\lambda_{De}}$

Sheath extends $\gtrsim 10\,\lambda_{De}$

non neutral region

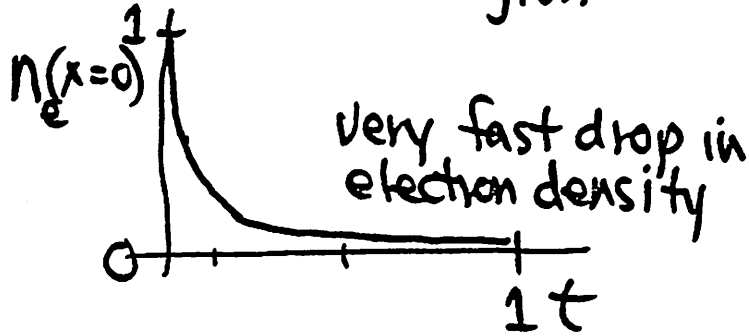

4%

2%

$n - n_e$ 0

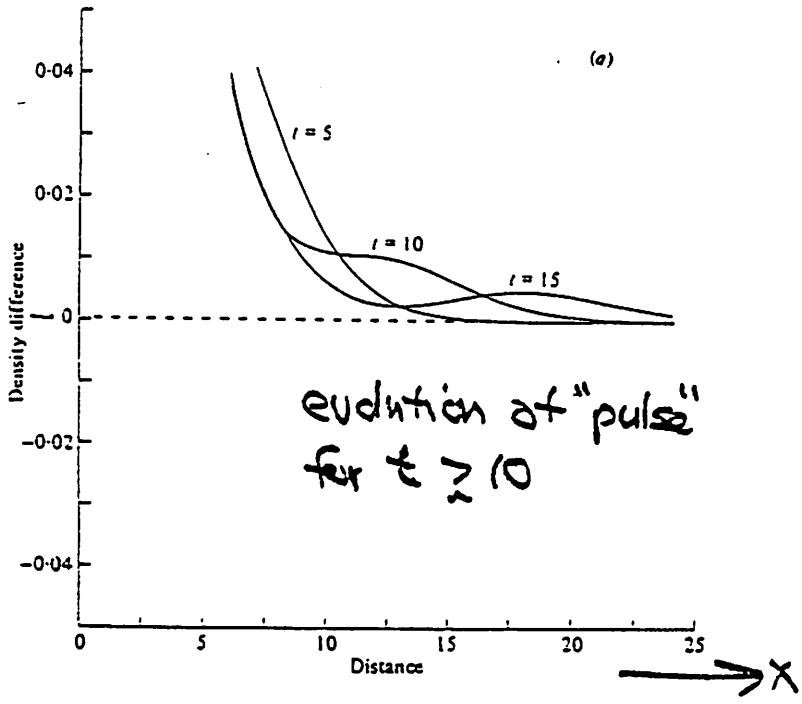

evolution of "pulse" for $t \gtrsim 10$

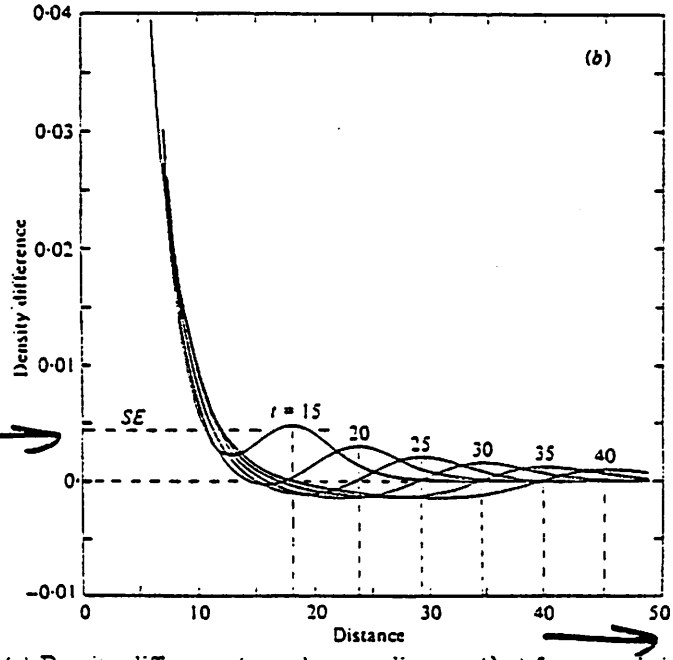

$n - n_e$

v_g of pulse decelerates toward v_s, pulse spreads; so, inconsistent with linear ion-acoustic dispersion.

"Sheath edge"

$\Delta n = 0.4\%$

FIGURE 5. (a) Density difference ($n - n_e$) *versus* distance (λ_{De}) for several times during the initial stages of the formation and expansion of the quasi-neutral region. (b) Density difference ($n - n_e$) *versus* distance (λ_{De}) for several times during the intermediate and later stages in the development of the quasi-neutral region. The line labelled *SE* marks the empirically derived density difference value that specifies the sheath edge data curve $\xi(t)$ (see text).

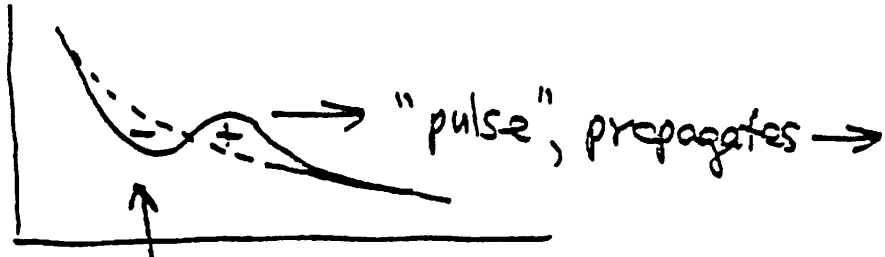

serves as pre-sheath accel. domain for cold ions.